UCRL-3785

UNIVERSITY OF CALIFORNIA

Radiation Laboratory

TWO-WEEK LOAN COPY

This is a Library Circulating Copy which may be borrowed for two weeks. For a personal retention copy, call Tech. Info. Division, Ext. 5545

BERKELEY, CALIFORNIA

DISCLAIMER

This document was prepared as an account of work sponsored by the United States Government. While this document is believed to contain correct information, neither the United States Government nor any agency thereof, nor the Regents of the University of California, nor any of their employees, makes any warranty, express or implied, or assumes any legal responsibility for the accuracy, completeness, or usefulness of any information, apparatus, product, or process disclosed, or represents that its use would not infringe privately owned rights. Reference herein to any specific commercial product, process, or service by its trade name, trademark, manufacturer, or otherwise, does not necessarily constitute or imply its endorsement, recommendation, or favoring by the United States Government or any agency thereof, or the Regents of the University of California. The views and opinions of authors expressed herein do not necessarily state or reflect those of the United States Government or any agency thereof or the Regents of the University of California.

UCRL-3785

UNIVERSITY OF CALIFORNIA

Radiation Laboratory
Berkeley, California

Contract No. W-7405-eng-48

I. THE INTERACTION OF NEGATIVE K MESONS AT REST IN COMPLEX NUCLEI
II. THE K^- MASS, Σ^- MASS AND $\Sigma^- - \Sigma^+$ MASS DIFFERENCE

Francis Henry Webb, Jr.

(Thesis)

May 1957

Printed for the U. S. Atomic Energy Commission

ABSTRACT

A study of the interaction of negative K mesons at rest in complex nuclei by the photographic emulsion technique has been made.

An unbiased sample of 133 K^- absorption stars has been found by the "along the track scanning method".

The observed stars are all consistent with the primary K^- absorption process by the strangeness conserving reactions K^- "N" $\rightarrow Y\pi$ and K^- "NN" $\rightarrow$ YN. The single nucleon absorption process in complex nuclei is predominant.

Calculated pion and hyperon spectra for the $K^-N \rightarrow Y\pi$ reactions occurring within complex nuclei are compared with the compilation of K^- absorption stars presented at the Sixth Annual Rochester Conference and they agree.

The calculated spectra are based upon the Serber optical model and take into account the presence of particle nucleon potential wells.

The observed shift in the pion spectra of 30 Mev for the Σ reaction from the free nucleon case is interpreted as primarily due to binding effects (a) the atomic binding of the K^- meson before absorption takes place, (b) the nuclear binding of the nucleon with which the K^- meson interacts.

The ratio of $K^-N^- \rightarrow \Lambda^0\pi$ to $K^-N^- \rightarrow \Sigma\pi$ has been determined as $.24 \pm .09$.

In $\sim$65% of the K^- absorption stars N^+ particles are emitted (which are presumably due to the primary process $K^-N^- \rightarrow \Lambda\pi$ and the secondary process $\Sigma^-N^- \rightarrow \Lambda N$).

The ratio of the K^-/K^+ masses has been determined by a range momentum method with the result $M_{K^-}/M_{K^+} = .998 \pm .013$. Several

events have been observed which are interpreted as the absorption of K^- mesons by the hydrogen of the emulsion by the reaction $K^- + H \rightarrow \Sigma^{\pm} + \pi^{\mp}$. These events allow an accurate determination of the K^-, Σ^- masses and the $\Sigma^- - \Sigma^+$ mass difference.

TABLE OF CONTENTS

	Page
Introduction	6
I. The Interaction of Negative K Particles at Rest in Complex Nuclei	9
A. Experimental Arrangement and Exposure	9
B. Technical Details	9
C. Scanning and Identification of Negative K Mesons	10
D. Experimental Analysis of K^- Absorption Stars	12
1. Prongs Classified as π Mesons	12
2. Slow Protons	14
3. Charged Hyperon Identification	14
E. Results	15
1. Prong Distributions	15
2. Frequency of Types of Absorption Stars	17
3. Total Visible Energy	20
4. List of Stars	22
F. Theoretical Discussion	30
1. Introduction	30
2. Allowed K^- "N" Reactions	32
3. Energy Spectra of Final State Products	36
G. Comparison with Experiment	53
1. π Spectrum with Associated Σ Hyperon	53
2. π Spectrum from all K^- Absorption Stars	55
3. Charged Hyperon Spectrum	63
4. Sum of Kinetic Energy of Σ Hyperon and Its Associated Charged Pion	66

Page

5. Total Energy Released 68

Appendix 72

References for Part I 75

II. The K^-, Σ^- Masses and the $\Sigma^- - \Sigma^+$ Mass Difference 76

A. Ratio of K^- Mass to K^+ Mass 76

B. The K^-, Σ^- Masses and the $\Sigma^- - \Sigma^+$ Mass Differences (from $K^- H \rightarrow \Sigma^{\pm}\pi^{\mp}$) 79

INTRODUCTION

The first example of the nuclear absorption of a negative K meson at rest was observed by Leprince Ringuet.[1] From the early examples it was apparent that in the majority of events the total visible energy was considerably less than the rest energy of the K^- meson, and evidence was presented which showed that the K^- nuclear absorption process could involve the formation of pions and hyperons.[2]

Phenomenological schemes to account for the properties of hyperons and heavy mesons have been proposed by Nishijima, Gell-Mann, and others.[3] These schemes involve the introduction of a new quantity called " strangeness " by Gell-Mann, which acts like a new quantum number. There is now substantial evidence in support of the main features of these schemes.

According to these schemes the K^- meson can interact with a nucleon to form a Y,π pair , and with two nucleons can form a Y,N pair.

With the completion of high energy accelerators in the billion electron volt range, it has become possible to produce K^- mesons in fair intensity and under controlled conditions. Consequently we have undertaken an experimental program to study the properties of negative K mesons and their interactions with complex nuclei by the photographic emulsion technique.

All published K^- absorption events in complex nuclei at rest, including the events reported here can be interpreted in terms of the strangeness conserving reactions K^- "N" $\rightarrow Y,\pi$,and K^- "NN" $\rightarrow$ Y,N. It must be remarked that many of the K^- absorption events observed in nuclear emulsion are complicated, and it is virtually impossible to make strong

arguments concerning the primary K^- absorption reaction in all individual cases.

Part I of this thesis contains a report on a study of the interaction of negative K mesons at rest in complex nuclei.

The K^- absorption stars at rest in complex nuclei have been observed to have the following properties:

1. The emission of charged hyperons and hyperfragments.
2. The emission of charged pions which sometimes occur in association with the emission of a charged hyperon.
3. The emission of high energy protons (30 - 200 Mev.)
4. The emission, in the majority of events, of low energy protons and prongs characteristic of evaporation processes.
5. The formation of zero pronged stars.
6. Many cases where the total visible energy is small enough to permit the emission of neutral hyperons. (Λ^0 & Σ^0)
7. A small number of cases where the total visible energy is so large that the hyperon must have been trapped and exploded inside the nucleus.

These experimental results are in agreement with similar work carried out concurrently by other groups [4].

We have calculated the pion and hyperon energy spectra for $K^- N'' \rightarrow \Sigma \pi$ and $K^- N'' \rightarrow \Lambda^0 \pi$ reactions occuring in complex nuclei on the basis of a simple optical model and have compared them with the experimental spectra and good agreement is obtained.

The single nucleon absorption process in complex nuclei is the most frequent reaction and proceeds mainly through the $\Sigma \pi$ mode.

In Part II of this thesis are described determinations of the masses of the K^- meson and Σ^- hyperon.

The ratio of the masses of the K^- to the K^+ mesons has been measured by a range momentum technique with the resulting value of $M_{K^-}/M_{K^+} = .998 \pm .013$.

Several events have been observed which are interpreted as the K^- meson absorption at rest by the hydrogen of the emulsion by the reactions $K^- + H \rightarrow \Sigma^{\pm} + \pi^{\mp}$. These events permit an accurate determination of the K^-, Masses and establish a $\Sigma^- - \Sigma^+$ mass difference.

I. The Interaction of Negative K Particles at Rest in Complex Nuclei

A. EXPERIMENTAL ARRANGEMENT AND EXPOSURE

A schematic diagram of the Bevatron exposures is shown in Figure 1. Protons of 6.2 Bev. kinetic energy are incident on a plunged target (Cu ½"x1"x1") placed in the west tangent tank, where the stray field of the Bevatron is low (< 100 gauss). The particles produced at 90° to the incident proton beam pass through a thin window (.090" Al.) on the west side of the Bevatron vacuum tank. These particles are then focused by four 2"x2" aperture strong-focusing quadropole magnets.[5] The particle sign and momentum interval are selected by a steering magnet placed behind the quadropoles. This beam then enters a stack of stripped emulsions. The emulsion stacks were placed so that the plane of the individual pellicles were verticle. The target to emulsion path was 3.2 meters and the momentum interval of the exposures was from 270 to 385 Mev./c, with a momentum dispersion of ± 5%.

Three stacks of Ilford G-5 600 micron stripped emulsion were exposed to this beam.

The proton flux on the target was measured by use of the induction electrode, and the exposures were limited to approximately 10^{13} protons on the target.

B. TECHNICAL DETAILS

The procedures used in preparing the stacks, development, and final pellicle processing have been described by Goldhaber ,et. al.[6] and Shapiro and Stiller[7]. The standard variable temperature Bristol development was used.

NOTE: For Fig. 1, see Part II.

C. SCANNING AND IDENTIFICATION OF NEGATIVE K MESONS

The negative K mesons were found by the "along the track scanning technique". This type of scanning introduces no bias in the type or size of ending found.

For the momentum interval in the exposures (270 to 385 Mev/c) particles of the τ mass possess an ionization relative to minimum [8] of from 2.0 to 2.7 at the leading edge of the pellicles, which is easily distinguished from the ionization of beam π mesons and lighter mass beam particles. We were able to determine the relative ionization and potential range of τ mass particles from the known dispersion of the magnetic system.[9]

The momentum dispersion (± 5%) was small enough that τ mass particles possessed a fairly well defined range. An experimental check of the momentum dispersion was obtained from the K^-/K^+ mass ratio exposure.[10] For the center pellicle in this exposure a momentum of 314 ± 6 Mev./c was obtained., which corresponds to an emulsion range of 4.25 ± .25 cm. for τ mass particles.

The angular spread of the beam was defined in both projected and dip angles to better than 10° with respect to the mean π direction.

For a track to be classed as a stopping K^- meson , it had to fit three criteria:

1. The relative ionization of the track at the leading edge of the pellicle had to be within ± .2 of the calculated value.
2. The track had to form an angle of < 10° in both dip and projected with respect to the mean π direction.
3. The range of a stopping track had to be within ±3/4 cm. of the calculated range.

Tracks which fall within these three criteria have been classified as stopping K^- mesons, unless the track ends without the formation of a visible absorption star, in which case the track underwent further analysis.

These three criteria are sufficiently severe to eliminate π mesons and lighter mass particles of any incident momentum from the sample.

In cases where there might have been a doubt a more accurate grain count was performed at several different residual ranges and identification was made on this basis.

The three criteria are not sufficiently strict to separate protons from K^- mesons forming zero pronged stars in all cases. Further measurements were made on this type of track. A grain count of at least 500 grains or a per cent opacity count was made on about the same length of track at several different residual ranges about a centimeter apart. Several of the tracks separated by these techniques were checked by multiple scattering measurements (constant sagitta versus residual range) and the identifications agreed. Not all of the tracks forming zero pronged stars (K^-_ρ candidates) were analyzed, and we have inferred from these unanalyzed tracks several additional K^- tracks. In one region of the stacks all K^-_ρ candidates were analyzed, so that in this region we have the measured ratio of K^- tracks forming visible absorption stars (at least one prong of range $> 10\mu$) to K^- tracks forming zero pronged events (tracks forming zero pronged stars, blobs, recoils, and prongs less than 10μ), we assume that this ratio is a constant. In the region where the K^-_ρ candidates have not been analyzed and since we knew the number of tracks forming K^- absorption stars we have inferred five additional K^-_ρ's on this basis.

D. EXPERIMENTAL ANALYSIS OF K^- ABSORPTION STARS

After a track was classified as a stopping K^- meson an analysis of its ending was made.

The following definitions were adopted:

Prong - - any series of grains which has a definite direction.

Recoil - - any prong whose length is less than or equal to 5

Blob - - any conglomeration of three or more grains which has no definite direction.

Prongs of all ionizations and widely varying ranges are emitted from K^- stoppings. In order to minimize the chance of missing a prong at least two observers carefully inspected each K^- stopping under 100x10 or 100x15 magnefication. The efficiency for seeing light prongs(g/g_o 1.5) is $> 90\%$ and for heavy prongs is $\sim 100\%$. Similarly each prong ending was carefully inspected , and the same efficiencies apply for observing decays and interactions of the prongs.

All prongs were followed as far as possible. Of the 306 prongs (excluding recoils) emitted from the 138 K^- stars, 38 were not followed to the end of their range, of these 15 were shower particles ($g/g_o \lesssim 1.4$) 15 had ionizations between 1.4 and 5, and 8 were black ($g/g_o \gtrsim 5$).

Range and ionization measurements, and characteristic endings were used in determining the identity and energy of each prong. The range-energy tables of Barkas and Young [11] were used.

1. Prongs classified as π^* mesons

33 of the 138 K^- absorption stars emitted prongs classified as mesons. (no case of double pion emission was observed.)

13 of these tracks were arrested in the emulsion so that charge and a good energy determination was obtained.

On 6 of the prongs it was possible to perform two grain counts at a great enough distance apart to permit a reliable identification and a good energy determination.

On the remaining 14 prongs only one grain count or estimate was possible. 5 of these prongs were emitted with a $g/g_0 < 1.3$ which rules out the possibility that the prongs are protons from energy consideration. 9 prongs were emitted with g/g_0 between 1.3 and 1.6 , and in these cases we cannot rule out conclusively the possibility that these prongs are protons. These 9 prongs have been classed as $\pi^{\pm}$ mesons since:

a. The highest energy of an identified proton was only 190 Mev. ($g/g_0 = 2.4 \pm .12$).

b. In all 12 cases where tracks were emitted with $g/g_0 < 2$, and where it was also possible to subsequently identify the track; they were all L mesons.

The possibility that some of these prongs are electrons or μ mesons is unlikely, since the K^- meson is a long lived strongly interacting particle. A strongly interacting K^- meson will only very rarely produce electrons or μ mesons as a result of the nuclear absorption of the K^- meson due to the extremely weak e and μ coupling to the nucleus. The emission of e or μ mesons due to the decay of a K^- meson at or near rest is also a rare process. Estimates indicate that the K^- meson will spend of the order of or less than 10^{-11} sec. (from the point where the track appears to be at rest) before nuclear absorption takes place in nuclear emulsion. Since the lifetime of the K^- meson is $\sim 10^{-8}$ sec.(12) very few of the K^- stoppings will be due to the decay process ($\lesssim .1\%$).

2. Slow Protons

All prongs in the range interval 5 μ to 3.5mm. were classed as slow protons unless identified as another particle or visually classed as an α particle.

In this range interval the contribution of d, t, and α particles is no doubt significant and even the visually identified α are an underestimate. No serious attempt was made to obtain a more reliable separation. The effect of incorrectly classifying d, t, and α as protons is to underestimate the kinetic energy of the prong, and will usually cause an underestimate of the total prong energy (kinetic energy plus binding energy).

Estimates of the total energy emitted in heavy particles (charged heavy particles and neutrons) was carried out in the same fashion as in the antiproton star analysis [13], and compensates for this underestimate.

3. Charged Hyperons Identification

Charged hyperons were identified by their characteristic endings.

At rest positive hyperons decay into either a proton with a range of 1650 $\pm$ 50 μ or into a minimum secondary (π^- meson).

Particles of nucleonic mass which form visible absorption stars when arrested in the emulsion were classified as Σ^- particles. If an electron was associated with the ending of a track of nucleonic mass, these tracks were also interpreted as Σ^- hyperons.

In flight Σ^+ hyperons decay either into a proton or a π meson and Σ^- hyperons decay into π mesons. Tracks which fit these conditions (and kinematics) have been classed as charged hyperon decays in flight.

E. RESULTS

1. Prong Distributions

The prong distributions have been plotted excluding recoil prongs ($\leq 5\mu$).

The prong distributions of all K^- stoppings is plotted in Figure 2. The average number of prongs is $2.3 \pm .25$.

The prong distribution of the K^- stoppings which emit a charged pion is plotted in Figure 3 (including the pion). The average number of prongs is $2.4 \pm .4$, and the average stable prong number is $1.3 \pm .4$

The prong distribution of those K^- stars which emit a charged hyperon is plotted in Figure 4 (including the hyperon). The average number of prongs is 2.6 ± 6, and the average number of stable prongs is $1.1 \pm .3$

The total prong distributions are the same within statistics indicating a higher average excitation energy in those K^- stars where no charged unstable particle is emitted.

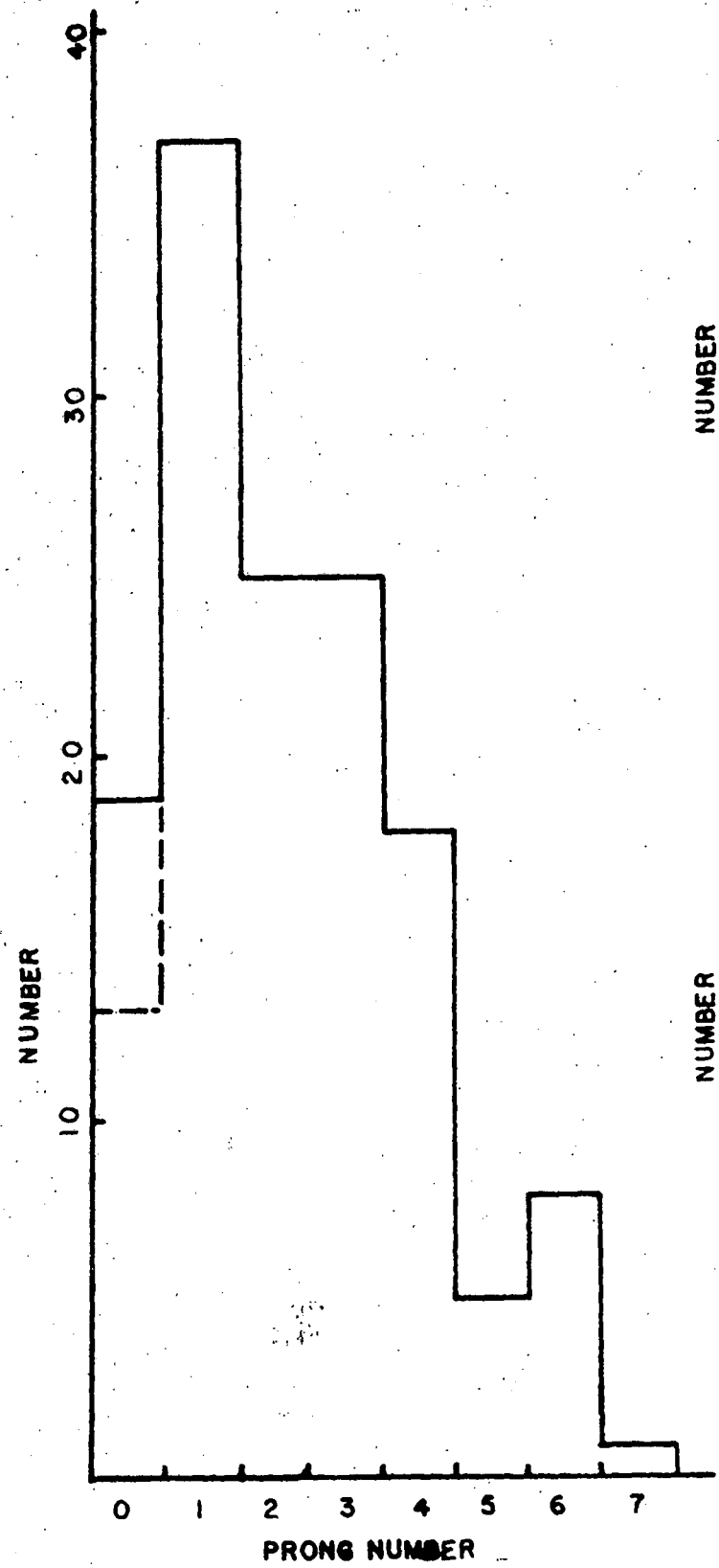

FIGURE 2, All K^- absorption stars.

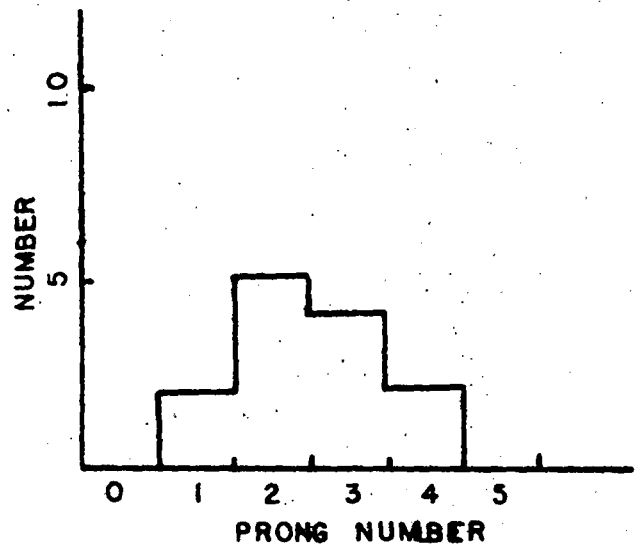

FIGURE 4, K^- absorption stars in which a charged hyperon is emitted (including the hyperon).

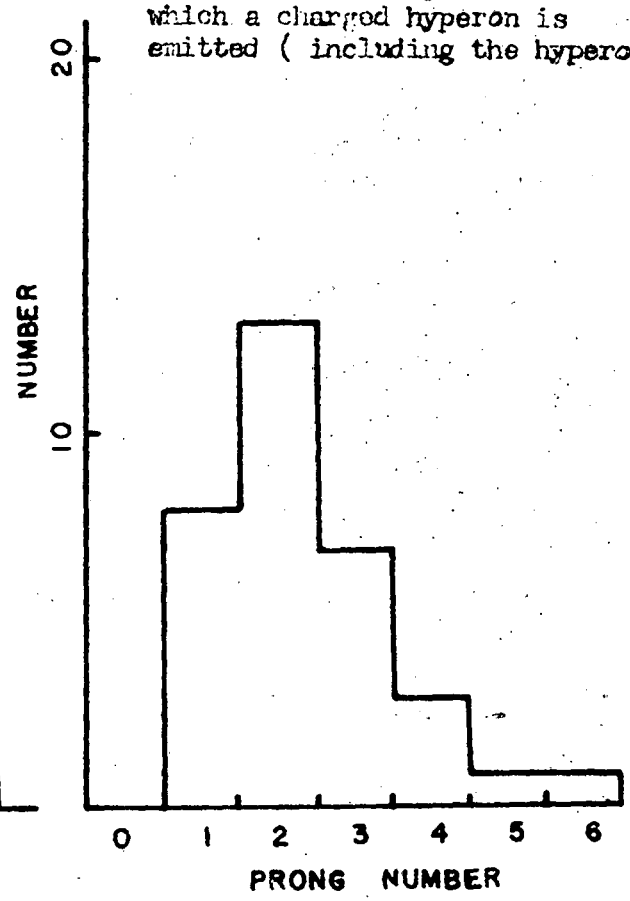

FIGURE 3, K^- absorption stars in which a charged pion is emitted (including the pion).

Figures 2 - 4 PRONG DISTRIBUTIONS FROM K^- ABSORPTION STARS WITHIN COMPLEX NUCLEI (excluding recoils 5)

2. Frequency of Types of K^- Absorption Stars

The K^- absorption stars have been grouped into the following categories:

a. $\sigma_{\Sigma,\pi}$ — A K^- star which emits both a charged pion and an identified charged hyperon.

b. σ_{Σ} — A K^- star which emits an identified charged hyperon.

c. σ_{π} — A K^- star which emits a charged pion.

d. $\sigma_{HYPER,\pi}$ — A K^- star which emits a charged pion and a hyperfragment.

e. $\sigma_{HYPER.}$ — A K^- star which emits a hyperfragment.

f. σ_{p} — A K^- star which emits no identified unstable particles but one or more protons with kinetic energy, $T_p \geq 30$ Mev.

g. $\sigma_{ev.}$ — A K^- star which emits no identified unstable particles and only evaporation prongs, $T_p \leq 30$ Mev.

h. ρ — A K^- star which has no visible prongs $> 5\mu$.

Table II

Identified Charge of Unstable Particles Emitted from K^- Absorption Stars

$\sigma_{\pi\Sigma}$			
$\Sigma^+\pi^-$	$\Sigma^-\pi^+$	$\Sigma^-\pi^\pm$	$\Sigma^+\pi^\pm$
1	0	2	2

$\sigma_\Sigma + \sigma_{\pi\Sigma}$							
Σ^-				Σ^+			$\Sigma^\pm$
all	forming star	associated electron	other	all	decay $\Sigma^+(\pi)$ at rest	decay $\Sigma^+(p)$	
7	4	2	1	6+(1)	3	3+(1)	0

$\sigma_\pi + \sigma_{\pi\Sigma}$	
π^-	π^+
10	3

Table I

Frequency of Types of K^- Absorption Stars

	$\sigma_{\pi,\Sigma}$	σ_{Σ}	σ_{π}	$\sigma_{hyper,\pi}$	σ_{hyper}	$\sigma_{p>30Mev}$	σ_{ω}	ρ	Total
no.	5	9	28	0	3	34	41	14 ◆ (5)	138
%	4	7	20	0	2	25	30	14	100%

Type	no.	no.with 1p of T_p 30 Mev.	no.with 2p each with T_p 30 Mev.	no. with 3p each with T_p 30 Mev.	no. with evap. prongs only.	no.with no prongs
σ_{π}	28	2	1	0	17	8
σ_{Σ}	9	2	0	0	5	2
$\sigma_{\pi\Sigma}$	5	0	0	0	1	4
$\sigma_{p>30Mev}$	34	21	11	2	0	0

3. Total Visible Energy

In Figure 5 is plotted the total visible energy released in K^- absorption stars. The total visible energy released was computed in the following fashion:

1. To the observed kinetic energy of a proton was added 8 Mev to take account of nuclear binding.
2. To the observed kinetic energy of an α was added 4 Mev for binding energy.
3. To the observed hyperon kinetic energy was added the $Q + M_\pi c^2 = 250$ Mev.
4. To the observed pion kinetic energy was added 140 Mev for the pion rest energy.
5. To the kinetic energy of each hyperfragment was added the Q value $+ M_\pi C^2$ for the Λ^c particle $\sim$ 177 Mev.

This curve is not a precise description of the total visible energy released since not all of the $\pi^\pm$ which are emitted are observed, about 10% of the pions with $g/g_o < 1.4$ (> 70 Mev) are probably missed, and probably about 20% of the prongs classed as slow protons are in reality d, t or α particles. The observed average total visible energy is: $\bar{E}_{vis} = 135$ Mev. If we assume that 50% of the Σ^- and 10% of the charged pions above 70 Mev are missed, this would raise the total visible energy release to $\bar{E}_{vis} \cong 160$ Mev.

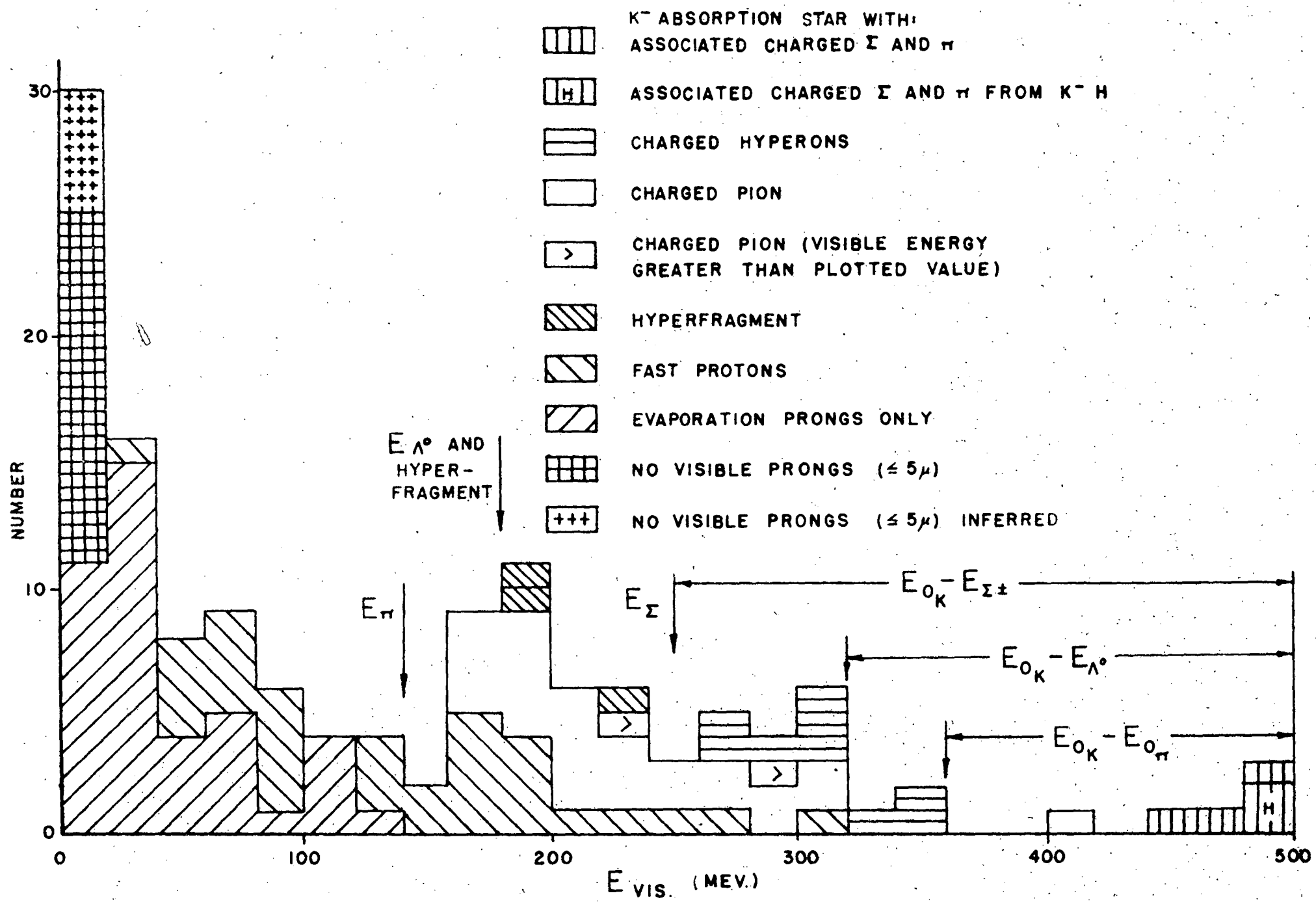

FIGURE 5. TOTAL VISIBLE ENERGY FROM K⁻ ABSORPTION STARS IN COMPLEX NUCLEI

4. List of Stars TABLE III

The quantities in each column are:

Column Number

1. Star Number
2. Type of Star
3. Number charged pions
4. Number of identified $\Sigma^{\pm}$ and hyperfragments emitted
5. Number of fast protons (Tp > 30 Mev) emitted
6. Number of evaporation prongs emitted
7. Kinetic energy of emitted charged pion
8. Kinetic energy of emitted $\Sigma^{\pm}$ hyperon or hyperfragment
9. Total kinetic energy in charged unstable particles observed
10. Total visible energy in star
11. Total energy in fast protons (including binding energy of 8 Mev for each fast proton)
12. Total energy in evaporation prongs (including binding energy of 8 Mev for each proton (p) and 4 Mev for each particle)
13. Kinetic energy of each fast proton
14. Kinetic energy of each evaporation prong.

Symbols used are:

b blob

p proton

alpha

r recoil

Energies are in Mev.

No	Type	N_π	N_Y	$N_{p>30}$	N_{ev}	σ_π	σ_Y	$\sum \sigma_{unst}$	$\sum \sigma_{vis}$	$\sigma_{p>30}$	$\sum \sigma_{ev}$	$\sigma_{p>30}$	σ_{ev}
1	$\sigma_{\pi 1}$	1				140^{+50}_{-25}		140	280				
2	$\sigma_{\pi 2}$	1				81^{+19}_{-13}		81	281				
3	$\sigma_{\pi 3}$	π^-				38		38	178				
4	$\sigma_{\pi 4}$	$1\pi^+$			a	44		44	184				
5	$\sigma_{\pi 5}$	1			b	150^{+150}_{-80}		~ 150	~ 290				
6	$\sigma_{\pi 6}$	$1\pi^-$			b	54		54	194				
7	$\sigma_{\pi 7}$	1			a	58^{+16}_{-12}		58	198				
8	$\sigma_{\pi 8}$	1			a	68^{+12}_{-16}		68	208				
9	$\sigma_{\pi 9}$	1			1	87^{+20}_{-16}		87	236		9		p1
10	$\sigma_{\pi 10}$	1			1,b	87^{+23}_{-14}		87	242		15		p7
11	$\sigma_{\pi 11}$	$1\pi^-$			1,b	47		47	206		19		p11
12	$\sigma_{\pi 12}$	$1\pi^+$			1,b	34		34	185		11		p3
13	$\sigma_{\pi 13}$	$1\pi^-$			1,b	14		14	167		13		p5
14	$\sigma_{\pi 14}$	$1\pi^-$			1,a	28		28	191		23		p15
15	$\sigma_{\pi 15}$	1			1,a	53^{+4}_{-4}		53	204		11		p3
16	$\sigma_{\pi 16}$	$1\pi^-$			1,a,b	27		27	178		11		p3
17	$\sigma_{\pi 17}$	1			1,2a	>65		>65	>225		20		α 26
18	$\sigma_{\pi 18}$	$1\pi^-$			2	50		50	214		24		p2 p6
19	$\sigma_{\pi 19}$	1			2	73^{+26}_{-18}		73	255		42		p6 p20
20	$\sigma_{\pi 20}$	$1\pi^-$			2	13		13	178		25		p4 p5
	Type	N_π	N_Y	$N_{p>30}$	N_{ev}	σ_π	σ_Y	$\sum \sigma_{unst}$	$\sum \sigma_{vis}$	$\sigma_{p>30}$	$\sum \sigma_{ev}$	$\sigma_{p>30}$	σ_{ev}

No.	Type	N_π	N_Y	$N_{p>30}$	N_{ev}	T_π	T_Y	ΣT_{unst}	ΣE_{vis}	$\Sigma E_{p>30}$	ΣE_{ev}	$T_{p>30}$	T_{ev}
21	$\sigma_{\pi 21}$	1			2 r	140^{+40}_{-30}		140	300		20		p3 p1
22	$\sigma_{\pi 22}$	1			2 r	83^{+37}_{-20}		83	265		42		p1 p25
23	$\sigma_{\pi 23}$	1 π^-		1	1 2r,b	37		37	231	41	13	p33	p5
24	$\sigma_{\pi 24}$	1			3	68^{+7}_{-5}		68	262		54		p10 p8 p12 p20
25	$\sigma_{\pi 25}$	1		1	2	48^{+5}_{-5}		48	285	70	27	p62	p14 p4
26	$\sigma_{\pi 26}$	1 -			3	13		13	210		57		p2 p7 p6
27	$\sigma_{\pi 27}$	1			4	80		80	297		77		p2 p3 p11 p10
28	$\sigma_{\pi 28}$	1		1	4	140^{+150}_{-50}		140	406^{+150}_{-50}	60	66	p52	p14 p7 p11 p5
29	$\sigma_{\pi\Sigma 1}$	1	1 $^+$( )			89	14	103	494				$K^- + H \to \Sigma + \pi$ collinear
30	$\sigma_{\pi\Sigma 2}$	1	1				12.6	99	494				* from Q
	$\sigma_{\pi\Sigma 3}$						30	87	477				$K^- + H \to \Sigma + \pi$, collinear
32	$\sigma_{\pi\Sigma 4}$	1	1 $^-_2$		r	65^{+3}_{-5}	3.3	68	458				
33	$\sigma_{\pi\Sigma 5}$	1	1 $^+$(p)		1,r	71^{+3}_{-3}	15	86	487		11		p3
34	$\sigma_{\Sigma 1}$		1 $^+$( )				62	62	312				
35	$\sigma_{\Sigma 2}$		1 $^+$(p)		4		29	29	279				
36	$\sigma_{\Sigma 3}$		1 $^+$( )	1	1		11	31	322	41		p33	
37	$\sigma_{\Sigma 4}$		1 $^-_3$		2,r		11	11	281		20		p3 p2
38	$\sigma_{\Sigma 5}$		1 $^+$(p)		2		4	4	274		20		p2 p2
39	$\sigma_{\Sigma 6}$		1 $^+$(p)		1		20 28	24	305		11		p6 p9
40	$\sigma_{\Sigma 7}$		1 $^-$(e)		2,r		32	32	307		35		p4 α_p
41	$\sigma_{\Sigma 8}$		1 $^-$(e)	1	2		6	6	353	42	35	p4 7	p6 α_{17}
No.	Type	N_π	N_Y	$N_{p>30}$	N_{ev}	T_π	T_Y	ΣT_{unst}	ΣE_{vis}	$\Sigma E_{p>30}$	ΣE_{ev}	$T_{p>30}$	T_{ev}

No.	Type	N_π	N_γ	$N_{p>30}$	N_{ev}	T_π	T_γ	$\sum T_{unst}$	$\sum E_{vis}$	$\sum E_{p>30}$	$\sum E_{ev}$	$T_{p>30}$	T_{ev}
42	$\sigma_{\leq 9}$		1 - 2		5		14	14	360		96		p6 p7 p4 p28 α15
43	σ_{Hyper1}		1					2Mev	180				
44	σ_{Hyper2}		1		r			2Mev	180				
45	σ_{Hyper3}		1		2			4Mev	236	54	54		α 8 α38
46	σ_{p1}			3	1				202	192	10	p63 p65 ±10 p40 ±5	α 6
47	σ_{p2}			3	1,r				319	299	20	p15 ±5 p39 p84	p12
48	σ_{p3}			2	5				178	93	85	p35 ±5 p42	p14 p6 p4 p16 p12
49	σ_{p4}			2	4				165	93	72	p40 ±5 p37	p8 p5 p20 α 8
50	σ_{p5}			2	3				185	142	43	p80 p46	p16 p2 p1
51	σ_{p6}			2	3,r				162	114	48	p58 p40	p13 p1 p10
52	σ_{p7}			2	4				267	168	99	p106 ±10 p46	p3 p14 p22 p28
53	σ_{p8}			2	1,r				158	148	9	p96 p36	p1
54	σ_{p9}			2	1				130	108	22	p47 p45	p14
55	σ_{p10}			2	r				197	197		p47 p34 ± 10	
56	σ_{p11}			2	0,b				222	222		p144 ±10 p62	
57	σ_{p12}			1	5				134	45	89	p37 ±7	p11 p9 p20 p2 p7
58	σ_{p13}			1	4				249	191	58	p183 ±19 -14	p6 p17 p2 p1
59	σ_{p14}			1	3				166	113	53	p113 ±10	α 17 p11 p5
60	σ_{p15}			1	3				134	65	69	p57	p4 p16 p25
61	σ_{p16}			1	3				93	39	54	p31	p3 p15 p11
No.	Type	N_π	N_γ	$N_{p>30}$	N_{ev}	T_π	T_γ	$\sum T_{unst}$	$\sum E_{vis}$	$\sum E_{p>30}$	$\sum E_{ev}$	$T_{p>30}$	T_{ev}

No	Type	N_π	N_τ	$N_{p>30}$	N_{ev}	T_π	T_Y	ΣT_{unst}	ΣE_{vis}	$\Sigma E_{p>30}$	ΣE_{ev}	$T_{p>30}$	T_{ev}
62	τ_{p17}			1	2,b				82	46	36	38	p1 p9
63	τ_{p18}			1	1,r				140	23	17	115±10	p8
64	τ_{p19}			1	2,b				91	46	45	38	p3 p16
65	τ_{p20}			1	2,b				68	44	24	36	p1 p7
66	τ_{p21}			1	2				85	46	40	38	p1 p4
67	τ_{p22}			1	2				90	72	18	64	p1 p1
68	τ_{p23}			1	r,r				40	40		32	
69	τ_{p24}			1	r,b				199	199		101±11	
70	τ_{p25}			1	r				46	46		38	
71	τ_{p26}			1	1				172	148	24	160±10	p6
72	τ_{p27}			1	r				68	68		60±5	
73	τ_{p28}			1	r,b				153	153		145±10	
74	τ_{p29}			1					39	39		31	
75	τ_{p30}			1	b				61	61		53	
76	τ_{p31}			1					76	76		68	
77	τ_{p32}			1					51	51		43	
78	τ_{p33}			1					54	54		46±3	
79	τ_{ev1}				4,3r				69		69		p18 p11 p10 p3
80	τ_{ev2}				6				308		308		p3 p4 p8 p14 p30 p26
81	τ_{ev3}				6,n				109		109		p18 p9 p3 p17 p4 p10
82	τ_{ev4}				6				127		127		p29 p21 p5 p5 p4 p15
No	Type	N_π	N_τ	$N_{p>30}$	N_{ev}	T_π	T_Y	ΣT_{unst}	ΣE_{vis}	$\Sigma E_{p>30}$	ΣE_{ev}	$T_{p>30}$	T_{ev}

o.	Type	N_π	N_Y	$N_{p\ 30}$	N_{ev}	T_π	T_Y	$\sum T_{unst}$	$\sum E_{vis}$	$\sum E_{p>30}$	$\sum E_{ev}$	$T_{p>30}$	T_{ev}
1	σ_{ev5}				5 b				97		97		p27 p8 p5 p10 p7
4	σ_{ev6}				4,r				54		54		p1 p5 p8 p8
5	σ_{ev7}				4,r				79		79		p11 p6 p6 p24
6	σ_{ev8}				4				101		101		p15 α19 p6 p24 p25
7	σ_{ev9}				4				72		72		p1 p4 p10 p25
8	σ_{ev10}				4				59		59		p4 p7 p8 p7
9	σ_{ev11}				4				78		78		p3 p20 p21 p1
0	σ_{ev12}				4 b				66		66		p19 p7 p7 p1
1	σ_{ev13}				4				118		118		p15 α 24 α 13 p13
2	σ_{ev14}				3,r				56		56		p7 p8 p17
3	σ_{ev15}				3				28		28		p2 p1 p1
4	σ_{ev16}				3				47		47		p21 p1 p1
5	σ_{ev17}				3				37		37		p5 p4 p4
6	σ_{ev18}				3				38		38		p1 p1 p12
7	σ_{ev19}				2,r				27		27		p10 p1
8	σ_{ev20}				3				31		31		p6 α 6 α 3
9	σ_{ev21}				2,r				24		24		p3 p5
00	σ_{ev22}				2,r				34		34		p3 p15
01	σ_{ev23}				2,b				35		35		p 9 p10
02	σ_{ev24}				1,r				18		18		α 14
o.	Type	N_π	N_Y	$N_{p>30}$	N_{ev}	T_π	T_Y	$\sum T_{unstt}$	$\sum E_{vis}$	$\sum E_{p>30}$	$\sum E_{ev}$	$T_{p>30}$	T_{ev}

Type	N_π	N_Y	$N_{p>30}$	N_{ev}	T_π	T_Y	ΣT_{inst}	ΣE_{vis}	ΣE_p	ΣE_{ev}	$T_{p>30}$	T_{ev}
ev25				2				10		8		p7 p5
ev26				1,r				25		25		p7
ev27				1,r				31		31		p
ev28				1,r				21		21		p3
ev29				1,r				26		26		p10
ev30				1,s				12		12		p
ev31				2,b				2		2		p6 p10
ev32				2,b				20		20		p4 p2
ev33				1				11		11		α 7
ev34				1,b				15		15		p
ev35				1				13		13		α 9
ev36				1				11		11		p3
ev37				1				9		9		p 1
ev38				1				17		17		α 13
ev39				1				19		19		p 11
ev40				1				7		5		p 29
ev41				1				10		10		p 2
P_1				2,r,5				0		0		
P_2				2				0				
P_3				2				0				
Tone	N_π	N_Y	N_p	N_{ev}	T_π	T_Y	ΣT_{inst}	ΣE_{vis}	ΣE_p	ΣE_{ev}	$T_{p>30}$	T_{ev}

No.	Type	N_π	N_γ	$N_{p>30}$	N_{ev}	T_π	T_γ	$\sum T_{mst}$	$\sum E_{vis}$	$\sum E_{p>30}$	$\sum E_{ev}$	$T_{p>30}$	T_{ev}
23	ρ_4								0				
24	ρ_5								0				
25	ρ_6								0				
26	ρ_7								0				
27	ρ_8								0				
28	ρ_9								0				
29	ρ_{10}								0				
30	ρ_{11}								0				
31	ρ_{12}								0				
32	ρ_{13}								0				
33	ρ_{14}								0				
No.	Type	N	N_γ	$N_{p>30}$	N_{ev}	T_π	T_γ	$\sum T_{mst}$	$\sum E_{vis}$	$\sum E_{p>30}$	$\sum E_{ev}$	$T_{p>30}$	T_{ev}

F. THEORETICAL DISCUSSION

1. Introduction

We will discuss the K^- absorption processes in complex nuclei in terms of the phenomenological schemes presented by Nishijima, Gell-Mann and others. (3) These schemes have been very successful in explaining the main properties of the hyperons and heavy mesons and their interactions with nuclear matter.

According to these schemes transitions which are allowed under the usual conservation laws may have quite different rates according to the degree to which a new quantity, called the "strangeness" by Gell-Mann, is conserved. Each elementary particle is assigned a strangeness number, S, and the strangeness of the system is defined as the algebraic sum of the strangeness numbers of the component particles. Also an intimate connection exists between the strangeness and the isotopic spin:

$$Q/e = I_3 + S/2 + N/2$$

where: Q/e is the charge number of the particle.

I_3 is the z component of isotopic spin of the particle.

S is the strangeness number of the particle.

N is the number of nucleons involved.

Table IV gives the assignments made by Gell-Mann and Nishijima.

Table IV

I \ S	-2	-1	0	+1
0	——	Λ^0 (0)	——	——
1/2	Ξ^-, Ξ^0	$K^-, \overline{K^0}$ (-1/2, 1/2)	n, p (-1/2, 1/2)	K^0, K^+ (-1/2, 1/2)
1	——	$\Sigma^-, \Sigma^0, \Sigma^+$ (-1, 0, 1)	π^-, π^0, π^+ (-1, 0, 1)	——

* The I_3 component is written directly beneath the particle.

The following rules are imposed on an interaction:

a. Q and N are always conserved.

b. For fast strong interactions (taking place in 10^{-23} sec. I, I_3, and S are conserved.

c. For electromagnetic interactions I_3, and S are conserved and $\Delta I = \pm 1$.

d. For weak interactions (taking place in 10^{-11} to 10^{-8} sec.) $\Delta S = \pm 1$,

e. For transitions $\Delta S > 1$

So slow that they are not observed.

2. Allowed K "N" Reactions

Applying these rules for a strong K^- nucleon interaction the following reactions are allowed:

(a) $K^- + p \longrightarrow \Sigma^+ + \pi^-$

(b) $K^- + p \longrightarrow \Sigma^0 + \pi^0$

(c) $K^- + p \longrightarrow \Sigma^- + \pi^+$

(d) $K^- + p \longrightarrow \Lambda^0 + \pi^0$

(e) $K^- + n \longrightarrow \Sigma^- + \pi^0$

(f) $K^- + n \longrightarrow \Sigma^0 + \pi^-$

(g) $K^- + n \longrightarrow \Lambda^0 + \pi^-$

(h) $K^- + N \longrightarrow Y + \pi + \pi$

and for the two nucleon absorption:

(i) $K^- + N + N \longrightarrow Y + N$

(j) $K^- + N + N \longrightarrow Y + N + \pi$

It should be noted that if no other selection rules are operative reactions (h and j) should be small from phase space considerations. We assume this to be so in the following discussion.

The branching ratios for the K^- single nucleon absorption reactions (a) to (g) can easily be derived by applying conservation of isotopic spin. Many authors have calculated these ratios [15], and the results are given in Table V.

Table V

Branching Ratios for $K^-N \to Y\pi$

Reaction Initial State	Final State	Matrix Element: (M. E.)
$K^-N \to \Sigma\pi$ $I = 1$	$I = 1$	$M_1 = a(\cos\theta + i\sin\theta)$
$K^-N \to \Sigma\pi$ $I = 0$	$I = 0$	$M_0 = b(\cos\phi + i\sin\phi)$
$K^-N \to \Lambda\pi$ $I = 1$	$I = 1$	$N_1 = c(\cos\omega + i\sin\omega)$

Reaction	Matrix Element (M. E.)	$(M.\ E.)^2$
(1) $K^- + p \to \Sigma^+ + \pi^-$	$\frac{1}{2} M_1 + \frac{1}{\sqrt{6}} M_0$	$\frac{1}{4} a^2 + \frac{ab\cos}{\sqrt{6}} + \frac{1}{6} b^2$
(2) $K^- + p \to \Sigma^0 + \pi^0$	$-\frac{1}{\sqrt{6}} M_0$	$\frac{1}{6} b^2$
(3) $K^- + p \to \Sigma^- + \pi^+$	$-\frac{1}{2} M_1 + \frac{1}{\sqrt{6}} M_0$	$\frac{1}{4} a^2 - \frac{ab\cos}{\sqrt{6}} + b^2/6$
(4) $K^- + n \to \Sigma^0 + \pi^-$	$-\frac{1}{\sqrt{2}} M_1$	$\frac{1}{2} a^2$
(5) $K^- + n \to \Sigma^- + \pi^0$	$\frac{1}{\sqrt{2}} M_1$	$\frac{1}{2} a^2$
(6) $K^- + p \to \Lambda^0 + \pi^0$	$\frac{1}{\sqrt{2}} N_1$	$\frac{1}{2} c^2$
(7) $K^- + n \to \Lambda^0 + \pi^-$	N_1	c^2

$\cos\alpha = \cos(\theta - \phi)$

Footnote:

In nuclear matter the K^- would be anticipated to interact predominantly with a single nucleon, to a lesser extent two nucleons, with larger aggregates even less frequently.

(1) For π^- absorption at rest in nuclear matter, it has been shown that the π^- is predominantly absorbed by a pair of nucleons in the nucleus [14] (Serber ( ), Puppi ( )).

When π^- interacts with a free nucleon at rest only the following processes are possible:

	(a) $\pi^- + N \rightarrow \pi^0 + N$	charge exchange (in nucleus - not possible from energy conservation)
	(b) $\pi^- + N \rightarrow \gamma + N$	electromagnetic
whereas	(c) $\pi^- + N \rightarrow N$	absorption (forbidden by momentum conservation)

When the absorption process is allowed by momentum conservation (i.e., when the interacts with two or more nucleons $\pi^- + N + N \rightarrow N + N$) the absorption process is the predominant mode. Hence crudely the would predominantly interact with a single nucleon in the nucleus, but the single nucleon channels are slower than the absorption process which requires at least two nucleons.

For the K^- meson, a strong K^- free nucleon process is possible $K^- + N \quad Y +$. If the Compton wavelength of the K^- is a rough measure of its interactive distance, then its sphere of interaction $(\lambda\!\!\!^{-}_{c K^-} / \lambda\!\!\!^{-}_{c \pi})^3$ is about 50 times smaller than the π^- sphere, so that the single nucleon reaction becomes plausible. The Pauli principle would inhibit the K^- from interacting with large aggregates of nucleons since after the interactions the remaining nucleons taking part in the interaction must go to unfilled states.

In a mixture of free nucleons the ratio of Λ^0 to $\Sigma^{\pm,0}$ particles produced is :

$$(\quad) \quad \frac{\Lambda^0}{\Sigma^{\pm,0}} = \frac{c^2(2\xi+1)}{a^2(2\xi+1)+b^2}$$

where ξ is the neutron to proton ratio.

The ratio of charged pions associated with Λ^0's from the $K^- N \to \Lambda^0 \pi$ reaction (designated as π_Λ^-) to charged pions associated with Σ particles from $K^- N \to \Sigma\pi$ reactions (designated as $\pi_\Sigma^\pm$) is given by:

$$\frac{\pi_\Lambda^-}{\pi_\Sigma^\pm} = \frac{3\xi c^2}{\frac{3a^2(1+\xi)}{2}+b^2}$$

When the n/p ratio is unity the $\frac{\Lambda^0}{\Sigma^{\pm,0}}$ ratio reduces to :

$$\frac{\Lambda^0}{\Sigma^{\pm,0}} = \frac{\pi_\Lambda^-}{\pi_\Sigma^\pm}$$

The ratio of $\pi_\Sigma^\pm$ to $\Sigma^\pm$ is unity and independent of the n/p ratio.

The ratio of neutral pions to charged pions from all the single nucleon reactions and neutral Σ^0 hyperons to charged $\Sigma^\pm$ hyperons is 1/2 when the n/p ratio is unity, i.e.

$$\frac{\pi^0}{\pi^\pm} = \frac{1}{2} \qquad \text{and} \qquad \frac{\Sigma^0}{\Sigma^\pm} = \frac{1}{2}$$

3. Energy Spectra of Final State Products

The kinetic energies of the final state products from the absorption at rest of a K^- meson with one and with two free nucleons are given in Table VI, (neglecting mass differences of n and p, $\pi^{\pm}$ and π^{0}, and Σ^{+} Σ^{-} and Σ^{0}).

TABLE VI

Final State Kinetic Energies from K^- Free Nucleon Absorption Reactions at Rest

Reaction	$K^- + N \longrightarrow Y + \pi$				
	Σ	π_Σ	Λ^0	π_Λ	
K. E. (Mev.)	15	90	27	150	
Reaction	$K^- + N + N \longrightarrow Y + N$				
	Σ	N_Σ	Λ^0	N_Λ	
K. E. (Mev.)	107	135	122	154	

The final state products from the reactions form line spectra composed of high energy pions and low energy hyperons for the single nucleon reaction, and high energy hyperons and nucleons for the two nucleon reaction.

When these absorption reactions take place within complex nuclei the line spectra of the final products will be spread out and shifted to lower energies. Not only are the reaction products formed with a spread of energies at lower energies, but the reaction products may interact before leaving the nucleus which will cause additional energy degration and attenuation of the spectra.

There are several effects which modify the line spectra when these reactions take place within nuclear matter.

a. Atomic binding

b. Primary Nuclear effects

i. Internal momentum of the nucleons in the nucleus.

ii. Binding of the nucleon in the nucleus.

iii. The presence of particle nuclear potentials in which the initial particle reacts and in which the final particles are formed and exist in until they leave the nucleus.

iv. Coulomb effects on the reaction products.

c. Subsequent interactions of the pions and hyperons as they leave the nucleus.

d. Subsidiary processes

i. Hyperfragment formation

ii. High energy nucleon emission in addition to the two nucleon process.

iii. Evaporation processes

iv. Decay of trapped Λ^{o} particles

(a) Atomic Binding

The K^- meson loses a small, but irreversible amount of energy to X-Ray and Auger electron emission in cascading to more tightly bound atomic orbits before nuclear absorption takes place.

The π^- meson is predominantly captured from 2 p or 3 d atomic states in heavy nuclei (Camac et. al) ( ). The atomic states from which K^- mesons are captured are not experimentally known, although calculations by Blatt and Butler ( ) indicate that the K^- meson is probably captured from a 2 p or higher atomic state in the heavy elements of the emulsion. For the same atomic state a K^- meson will be more tightly bound than a π^- meson due to the K^- meson's greater mass.

An estimate of the atomic binding of the K^- meson is the height of the Coulomb barrier, which is 4 Mev. for the light elements (C, N, O) of the emulsion, and 9 Mev. for the heavy elements (Ag,Br) of the emulsion.

(b) Primary Nuclear Effects

We will treat the K^- single nucleon-nucleus absorption reaction in terms of a simple optical model ( ).

A bound nucleon in the nucleon possesses kinetic energy with respect to its nucleon-nucleus potential well, and the K^- meson could also possess kinetic energy with respect to a K^- nuclear well. The K^- meson and bound nucleon interact within the nucleus, and it is here that momentum is conserved. The reaction products ($Y + \pi$) are formed in their respective particle - nuclear wells, and remain in them until they emerge from the nucleus.

In the accompanying diagram are shown the various potential wells and symbols used to describe the $K^- N \rightarrow Y\pi$ reaction.

Particle - Nucl Potential Wells

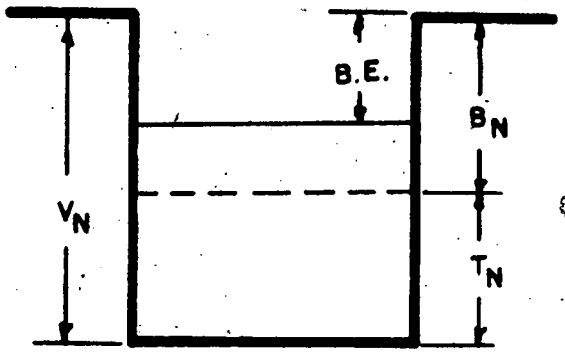

V_N = nucleon-nucleus well depth

B.E. = binding energy of last nucleon

B_N = binding energy of nucleon which interacts with K

T_{N_i} = kinetic energy of nucleon which interacts with K^-

Nucleon - Nucleus Well

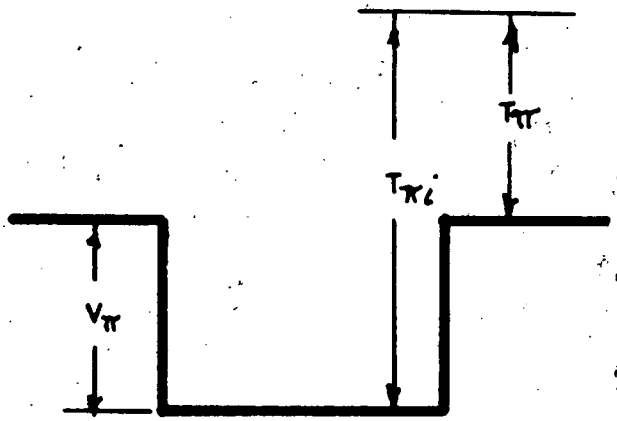

V_π = pion-nucleus well depth

T_{π_i} = kinetic energy of pion inside nucleus

T_π = kinetic energy of pion outside nucleus

Pion - Nuclear Well

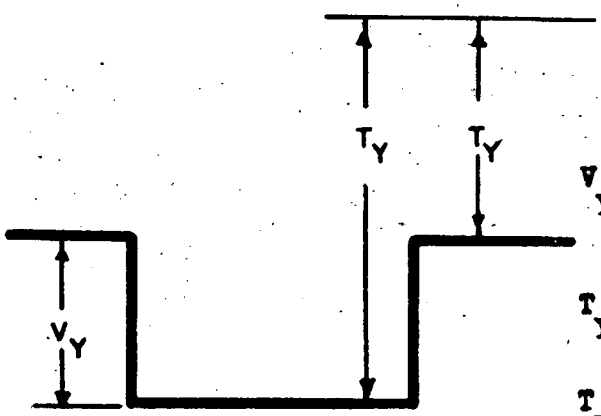

V_Y = hyperon-nucleus well depth

T_{Y_i} = kinetic energy of hyperon inside nucleus

T_Y = kinetic energy of hyperon outside nucleus

Hyperon - Nuclear Well

* Coulomb effects are neglected in these diagrams and the potential wells are considered as simple square wells.
Diagrams are not drawn to scale.

between the limits $\pm f$, where $f = p_{cm}\ \beta_{cm} / \sqrt{1-\beta_{cm}^2}$ and with a rectangular probability distribution $P = \frac{1}{2f}$

The new symbols are defined below:

$t_{\pi 1}$ = central value of the kinetic energy of the in the laboratory frame for a nuclear momentum of $\vec{p}_{M_1}$ and $\vec{p}_{K_1} = 0$

t_{Y1} = central value of the kinetic energy of the in the laboratory frame for a nuclear momentum of $\vec{p}_{M_1}$ and $\vec{p}_{K_1} = 0$

e_π^λ = total energy of π in center of mass frame, $\sqrt{M_\pi^2 + p_{cm}^2}$

e_Y^k = total energy of Y in center of mass frame, $\sqrt{M_Y^2 + p_{cm}^2}$

β_{cm} = the β of the center mass (velocity of center mass / velocity of light)

To obtain the spectra of the pions and hyperons inside the nucleus, the momentum distribution of the nucleons inside the nucleus and the cross section $\sigma_{K^- p \to Y\pi}$ must be folded into the above distribution.

We have assumed that the $K^- N \to Y\pi$ cross section is energy independent in the region ± 40 Mev. The hyperon and pion spectra have been calculated using both the Gaussian (i.e. value of 20 Mev) momentum distribution, and the Fermi momentum distribution ($T_{N,max}$ = 25 Mev).

To obtain the pion and hyperon spectra outside the nucleus the following transformations were made:

$$T_\pi = T_{\pi 1} + V_\pi$$

$$T_Y = T_{Y1} + V_Y$$

The pions are formed in an energy region where the pion-nuclear well depth is approximately constant [19], and we have used an energy independent value of -40 Mev. The hyperon nuclear well depth has been assumed to be energy independent and equal to -15 Mev.

The transformation of the number of particles in the energy interval T to T + dT from inside the nucleus to outside the nucleus is then

$$\left(\frac{dN}{dT}\right)_{outside} = \left(\frac{dN}{dT}\right)_{inside}$$

for corresponding energy values $(T_{outside} = T_{inside} + V)$.

The resulting pion and hyperon spectra outside the nucleus are shown in figures 6 and 7 . The pion spectra are normalized to equal amounts of $\pi_{\Sigma^-}^{+}$ and π_{Λ}^{-} production. There is a shift to lower kinetic energies for the central values of the pion spectra compared with the free nucleon reactions; The shift is 30 Mev. for the $\pi_{\Sigma^-}^{+}$ and 32 Mev. for the π^- .

The central values are:

$T_{\pi} = 60$ Mev. Σ, π process

$T_{\pi^-} = 118$ Mev. Λ^0, π process

The hyperon spectra extend over a wide energy range due to the effects of the internal momentum. The hyperons can also be produced with insufficient energy to get out of the nucleus due to the hyperon-nuclear potential well. And the hyperons produced with small energies sufficient to emerge from the nucleus can spend a longer time in the nucleus than the nuclear transit time due to the reflections at the nuclear surface, and these reflected hyperons possess a larger probability for nuclear interaction.

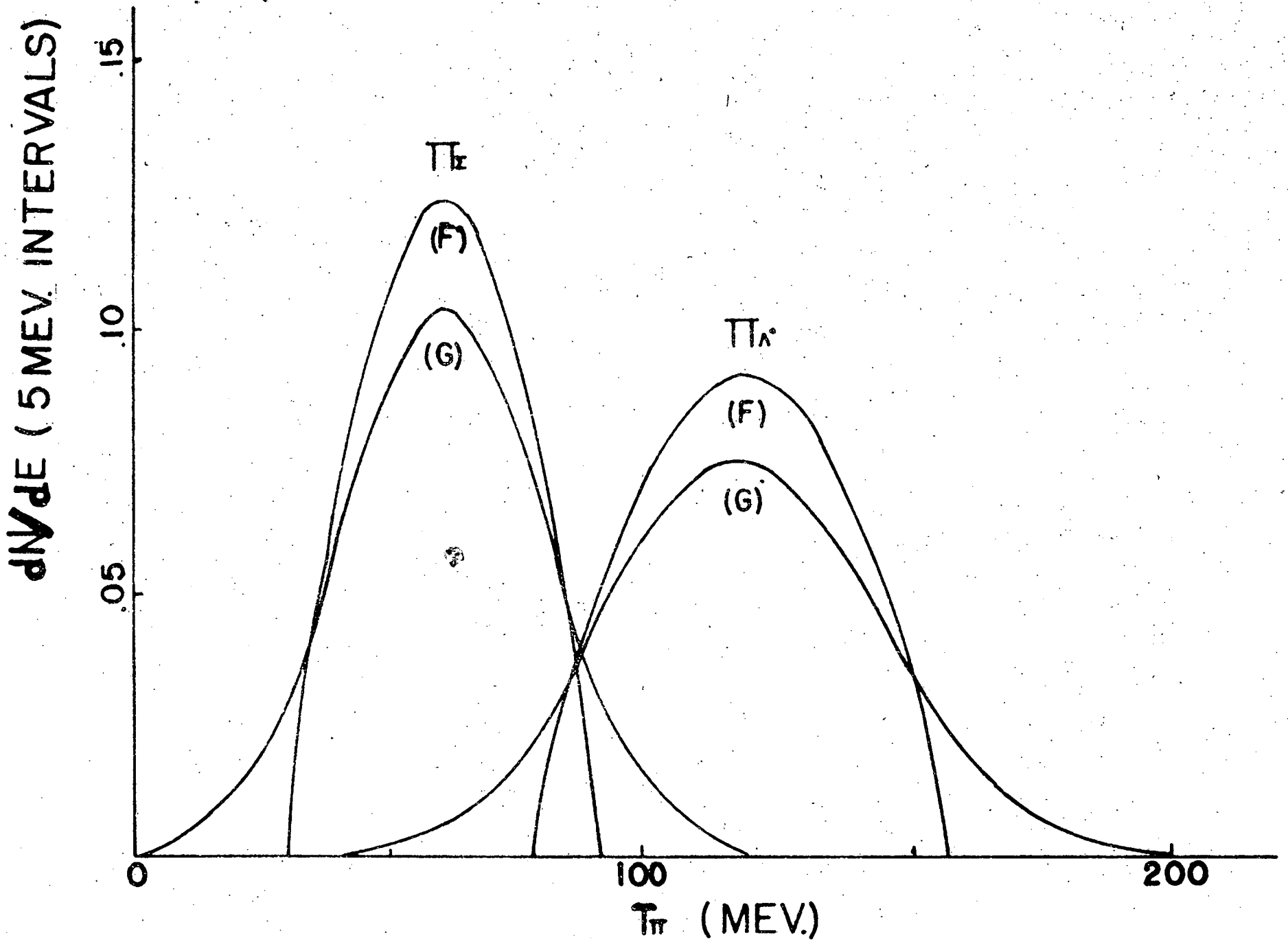

FIGURE 6. PION SPECTRA FOR $K^- "N" \longrightarrow Y\pi$

(G) USING GAUSSIAN DISTRIBUTION

(F) USING FERMI DISTRIBUTION

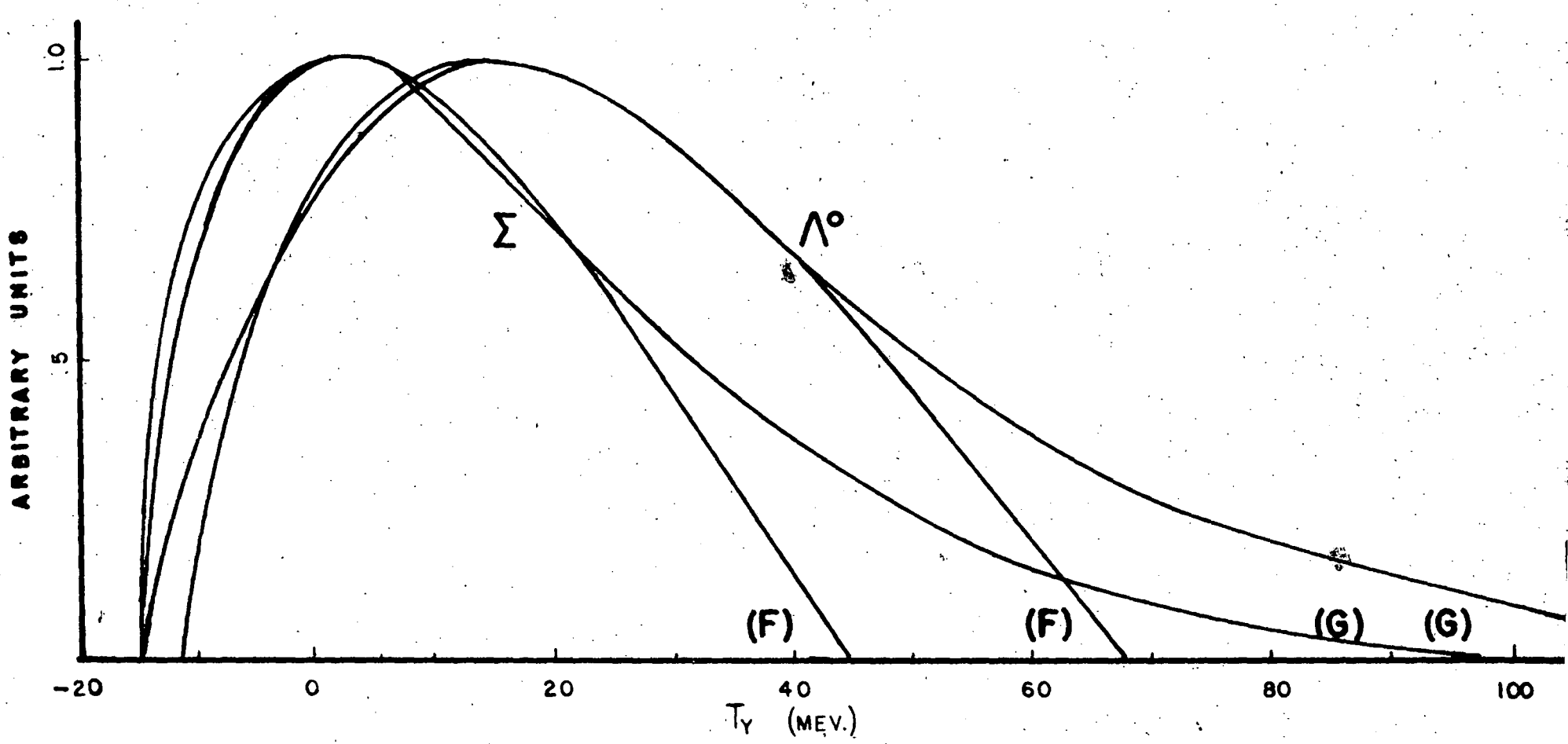

FIGURE 7, HYPERON SPECTRA: $K^-{}''N'' \rightarrow Y\pi$ ($V_Y = -15$ MEV.)

(neglecting Coulomb potential shifts)

(F) Using Fermi distribution

(G) Using Gaussian distribution

The depth of the hyperon well has little effect on the shape of the spectra, but the well depth will shift the spectra appreciably.

The Coulomb potential will make the Σ^- well deeper ($V_{\Sigma^-} + V_c$ with $V_c < o$) whereas the Coulomb potential will make the Σ^+ well shallower ($V_{\Sigma^+} + V_c$ with $V_c > o$) in addition to a low energy Coulomb cut off for the Σ^+ hyperons.

For a Coulomb potential of 6 Mev and equal hyperon potentials $V_{\Sigma^-} = V_{\Sigma^+} = -15$ Mev, the origin of the Σ^- spectrum will be $-15 - 6 = -21$ Mev below the zero energy outside the nucleus, whereas the Σ^+ origi n will only be -9 Mev below zero energy outside the nucleus.

(c) Estimate of Subsequent Interactions

(1) Pion Interactions

It is difficult to estimate the subsequent pion interaction in leaving the nucleus in which they were formed. We choose a simple model to make this estimate.

We assume that the K^- capture probability is constant per unit volume inside the nucleus (capture from S states) *. We then use an equation for uniform pion creation inside the nucleus derived by Bruckner, Serber, and Watson [20], which gives the fraction of mesons produced in a nucleus which are not absorbed in leaving the nucleus (f_a) in terms of the nuclear radius ($R = r_o A^{1/3}$) and the pion absorption mean free path, λ_a, within nuclear matter:

$$f_a = 3\left\{ \frac{1}{2x_a} - \frac{1}{x_a^3} + \frac{1}{x_a^3}\left(1 + x_a \right) \exp - (x_a) \right\}$$

where $x_a = 2R / \lambda_a$.

This equation is valid when the absorption mean free path, λ_a, is much smaller than the scattering mean free path, λ_s. This condition does not hold over the entire pion energy region of interest (0 - 180 Mev.). To treat the higher pion energy region (above ~ 50 Mev.) where $\lambda_s \lesssim \lambda_a$ we have replaced the total mean free path, λ_t, $\left(1/\lambda_t = 1/\lambda_a + 1/\lambda_s \right)$ and used $x_t = 2R / \lambda_t$ instead of the absorption mean free path, λ_a, and x_a, in the equation yielding the fraction of mesons emitted, and designated by the symbol f_t.

The effect of the scattering mean free path is to effectively enlarge the size of the nucleus. Hence the fraction f_a is the maximum amount of pion emission and f_t is the minimum amount of pion emission.

---

*Capture from S states will yield the maximum amount of pion absorption. Capture from 2 p states will result in a smaller amount of pion absorption and inelastic scattering in leaving the nucleus. Crude estimates indicate $\lesssim$ 10% less.

In Figure 8, Curve A is a plot of $\langle f_a \rangle$ using values of λ_a [21] and averaged over the emulsion constituents in proportion to the relative stopping powers and relative volumes of the gelatin and AgBr crystals (35% CNO and 65% AgBr); Curve B is a plot of $\langle f_t \rangle$ similarly averaged over the emulsion constituents and using values of λ_t [21]. The values of $\langle f_a \rangle$ (Curve A) and $\langle f_t \rangle$ (Curve B) bracket the true amount of pion emission for uniform pion creation within the nucleus.

From star studies of the pion-nuclear interaction in emulsion in the pion energy range 60 - 150 Mev. [22] about 25% of the pions which have undergone nuclear interactions and are re-emitted from the nucleus are inelastically scattered. Curve C is a plot of $F = \langle f_t \rangle + \frac{1 - \langle f_t \rangle}{4}$ where F is the estimated total amount of pion emission and is composed of two terms $\langle f_t \rangle$ the elastic contribution, and $\frac{1 - \langle f_t \rangle}{4}$, the inelastic contribution. Below a pion energy of 100 Mev. $\langle f_a \rangle$ is smaller than $\langle f_t \rangle + \frac{1 - \langle f_t \rangle}{4}$ due to the smaller effect of the scattering mean free path. In this region we have used for the estimate of the amount of inelastic scattering the difference between $\langle f_a \rangle$ and $\langle f_t \rangle$ (i.e. $\langle f_a \rangle - \langle f_t \rangle$).

The energy distribution of the inelastically scattered pions in the energy region 60 - 150 Mev. has been observed to be approximately independent of initial energy with a peak of inelastic pions at 30 Mev. For the estimate of the inelastic pion distribution we have used an average of the results of Bernardini, et. al. and Goldhaber, et. al. ( ) The effects of these modifications on the calculated pion spectra ($\pi_z^{\pm}$ and π_Λ^{-}) are shown in Figure 9.

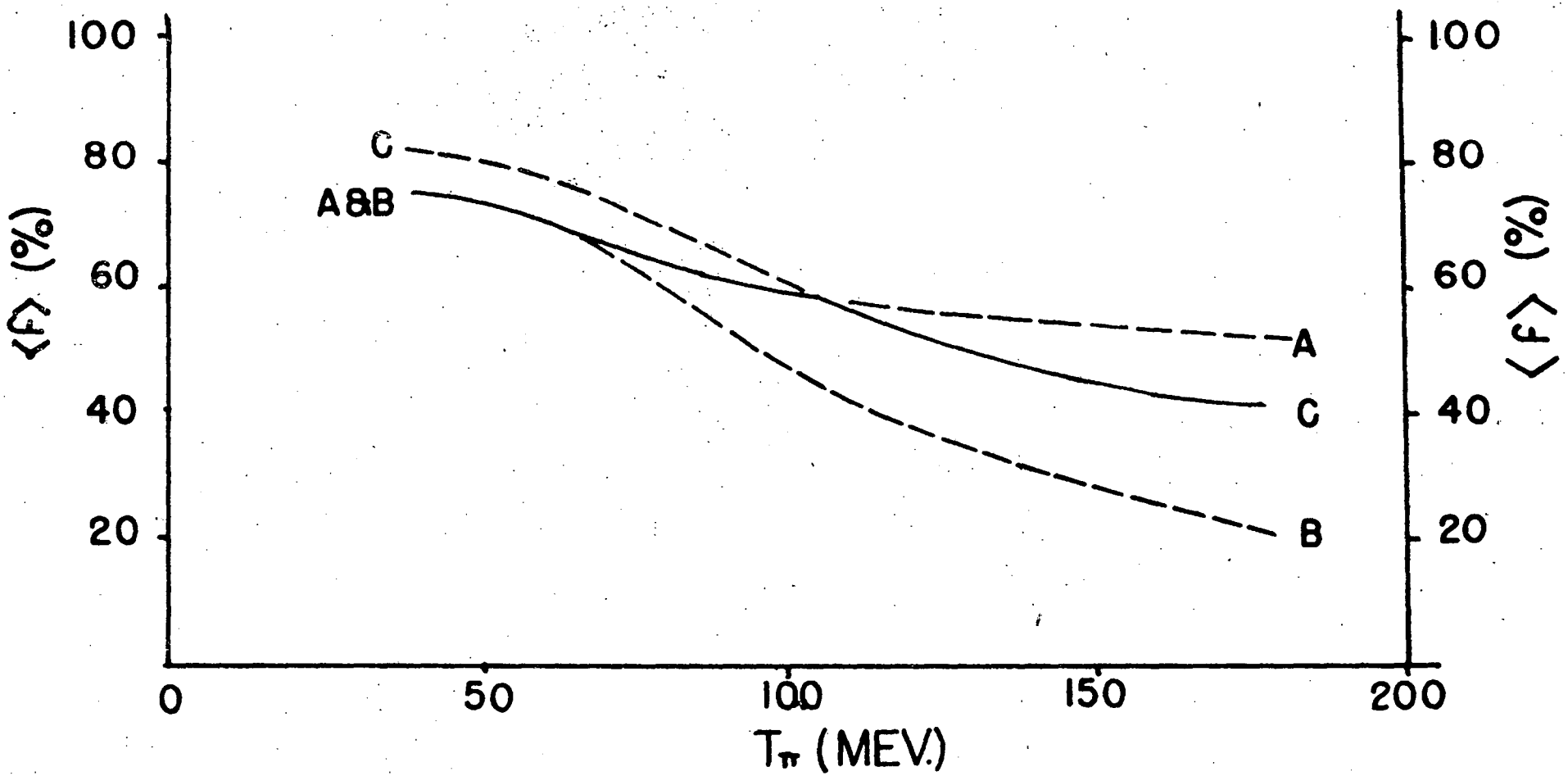

FIGURE 8 . Calculated pion emission frequencies (for homogeneous formation of pions)

Curve A fraction of pions not absorbed in leaving the nucleus, $\langle f_a \rangle$, using λ_a ; strictly valid only where $\lambda_a \ll \lambda_s$.

Curve B fraction of pions which have suffered no interaction in leaving the nucleus, $\langle f_t \rangle$, using λ_t (where $1/\lambda_t = 1/\lambda_s + 1/\lambda_a$)

Curve C fraction of pions which suffer no interaction in leaving the nucleus plus fraction which has undergone an inelastic scattering:

$$\langle f_t \rangle + \frac{1 - \langle f_t \rangle}{4}$$

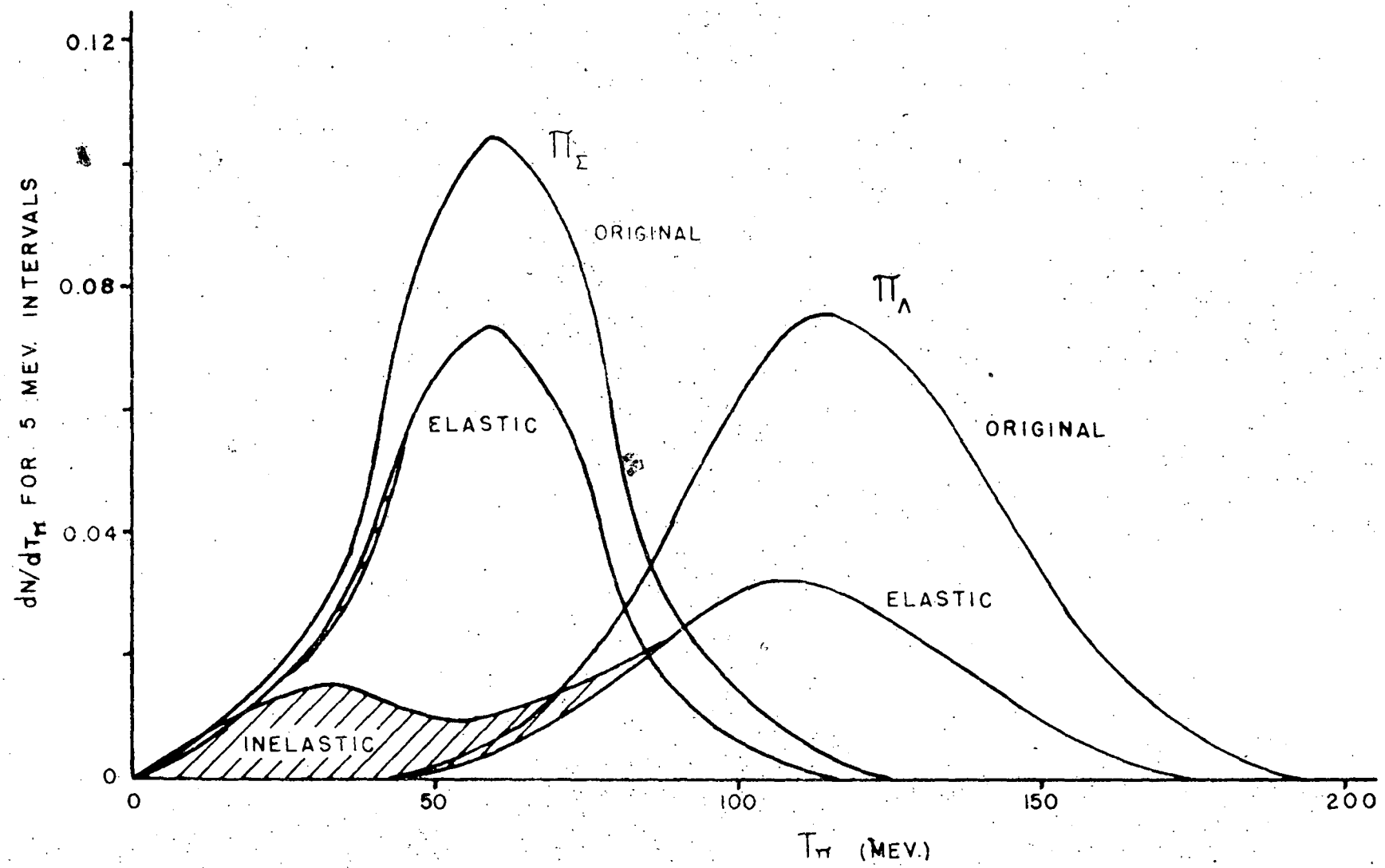

FIGURE 9. CALCULATED PION SPECTRA FOR K^- "N" $\rightarrow Y\pi$ WITH EQUAL PRODUCTION OF $\pi^{\pm}_{\Sigma}$ AND π^-_{Λ}

(c-2) Subsequent Hyperon Interaction

At the present time it is even more difficult to estimate the subsequent hyperon interactions before leaving the nucleus. This is mainly due to the meager knowledge of the nuclear interaction properties of the hyperons.

The Σ hyperons presumably interact with nucleons via:

$$\Sigma^{+} + n \rightarrow \Lambda^{0} + p \sim 72 \text{ Mev.}$$

$$\Sigma^{0} + p \rightarrow \Lambda^{0} + p \sim 72 \text{ Mev.}$$

$$\Sigma^{0} + n \rightarrow \Lambda^{0} + n \sim 72 \text{ Mev.}$$

$$\Sigma^{-} + p \rightarrow \Lambda^{0} + n \sim 72 \text{ Mev.}$$

The charge exchange reaction $\Sigma +$ "N" $\rightarrow \Sigma +$ "N" is presumably small due to phase space considerations. The nucleon interaction should yield Λ^{0} particles.

At the present time essentially no information is available on the inelastic scattering properties of the hyperons so that a discussion even as sketchy as that for the pions is not possible.

The interaction cross-sections of the Σ^{+} and Σ^{-} hyperons in nuclear matter should be equal when passing through nuclear matter equally populated by neutrons and protons.

The particle branching ratio Σ^{-}/Σ^{+} emitted should be nearly equal to the Σ^{-}/Σ^{+} ratio at formation if the neutron to proton ratio is near unity.

By applying the same approach used in estimating the amount of subsequent pion interaction we can calculate (using eq. ( )) the fraction of hyperons not absorbed in leaving the nucleus as a function of the absorption mean free path λ_a . In Figure 10 the results of this calculation are given averaged over the emulsion constituents.

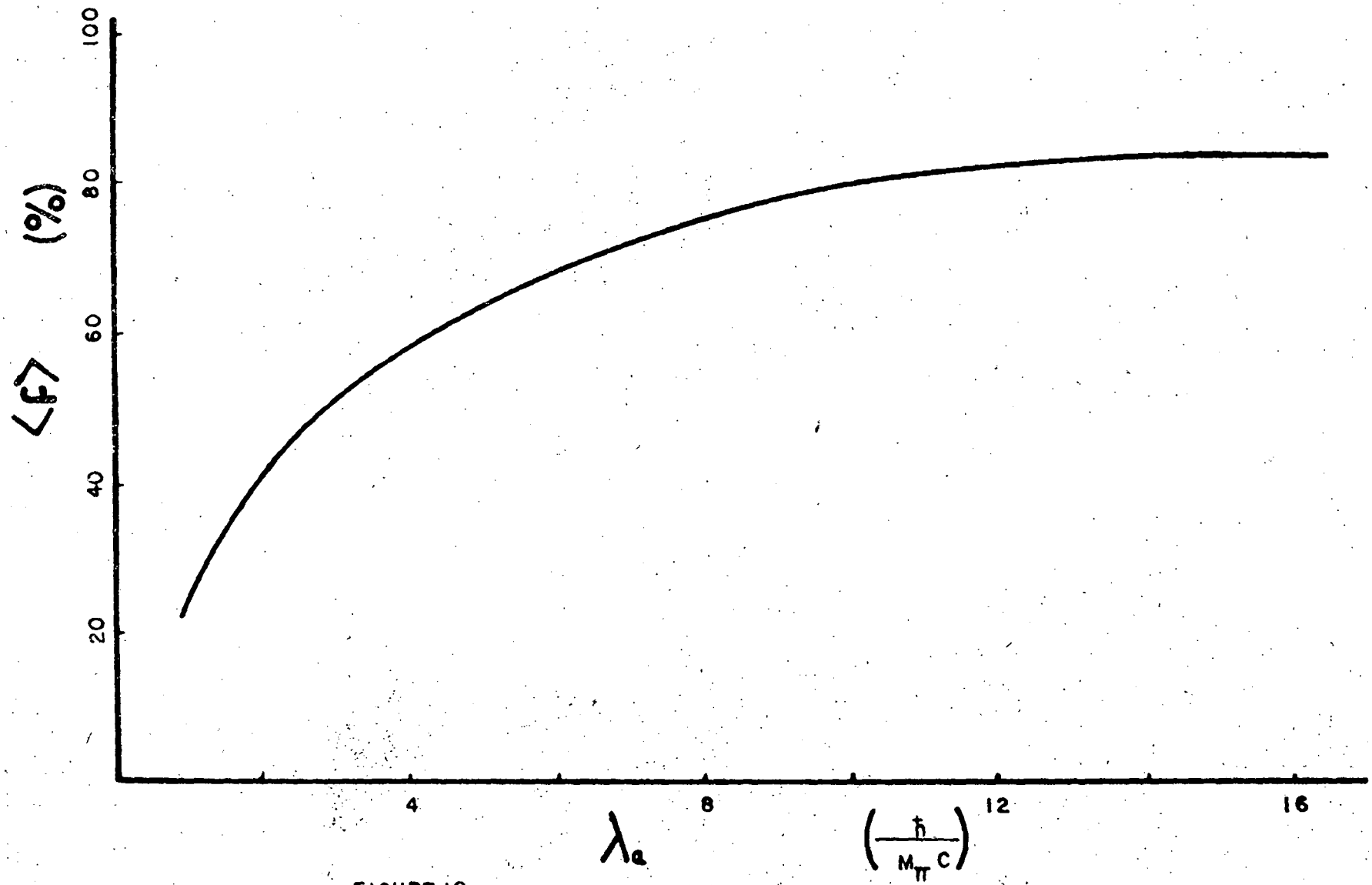

FIGURE 10, Attenuation of Σ hyperon emission frequency for various absorption mean free paths in units of the pion Compton wavelength (averaged over emulsion constituents).

(d) Subsidiary Processes

i. Hyperfragment formation

Hyperfragments would be formed as subsidiary processes and not as a result of the primary K^- nucleon absorption process. The hyperfragments would result from previously formed Λ^0 which become bound in nuclear fragments that are ejected from the nucleus. The Λ^0's arise from either the primary absorption process or the subsequent interactions of the Σ hyperons. The Σ hyperons which are created with insufficient energies to leave the nucleus will quickly undergo nuclear interactions forming Λ^0's (10^{-22} sec).

ii. Fast Nucleon formation:

Fast nucleon formation can result from the subsequent interaction of either Y or π or both before they leave the nucleus, which will take place in the order of 10^{-22} sec.

iii. Evaporation Spectra

Evaporation spectra composed of nucleons, heavier particles and perhaps even Λ^0 either bound or free (if the Λ^0 were trapped within the nucleus) will result from the excitation produced when the K^- absorption process occurs, and is increased when either one or both of the reaction products interact before leaving the nucleus. These processes will take place in -10^{-19} sec.

iv. Λ^0 Decay

If the Λ^0 hyperon is still within the residual nucleus it will decay either mesonically or non-mesonically in a time of $\sim 10^{-11}$ sec.

v. Since each time stage is separated by wide time intervals the conservation laws must be applied to each stage separately. In particular the energy available in each stage is limited.

(g) Comparison with Experimental Data

To obtain a large sample of data with which to compare the calculated spectra we will use the compilation of K^- absorption stars prepared by Sula Goldhaber for the Sixth Annual Rochester Conference ( ). This compilation includes published and unpublished data of several groups ( ): Hornbostel and Salant, Goldhaber et al, G. Stack Collaborators, Fry et al, George et al, White et al, and Schein et al.

1. $\pi^{\pm}$ Spectrum with Identified Associated $\Sigma^{\pm}$ Hyperon.

This experimentally determined pion spectrum is the pion spectrum from those K^- stars in which both an observed pion and identified $\Sigma^{\pm}$ hyperon are emitted. The energy determination of those pions below Mev. are quite accurate and the experimental errors (for the majority of events) are within the 20 Mev. intervals plotted in the histogram in Figure . The pion energies above 80 Mev. are in general less well determined since the energy determinations are based on grain count measurements. The experimental errors of these pions are generally greater than the 20 Mev. intervals used in plotting the histogram and we have used the measured energy and have not included any weighting factor for the errors of these measurements.

The calculated pion spectra for the $K^-N'' \rightarrow \Sigma\pi$ using both the Gaussian and Fermi distributions has been normalised to the experimental data on the basis of equating the area under the calculated spectra to the area of the histogram.

The agreement between the calculated spectrum using the Gaussian distribution and experimental histogram is very good. Both curves peak at 60 Mev. and have the same width. As would be anticipated

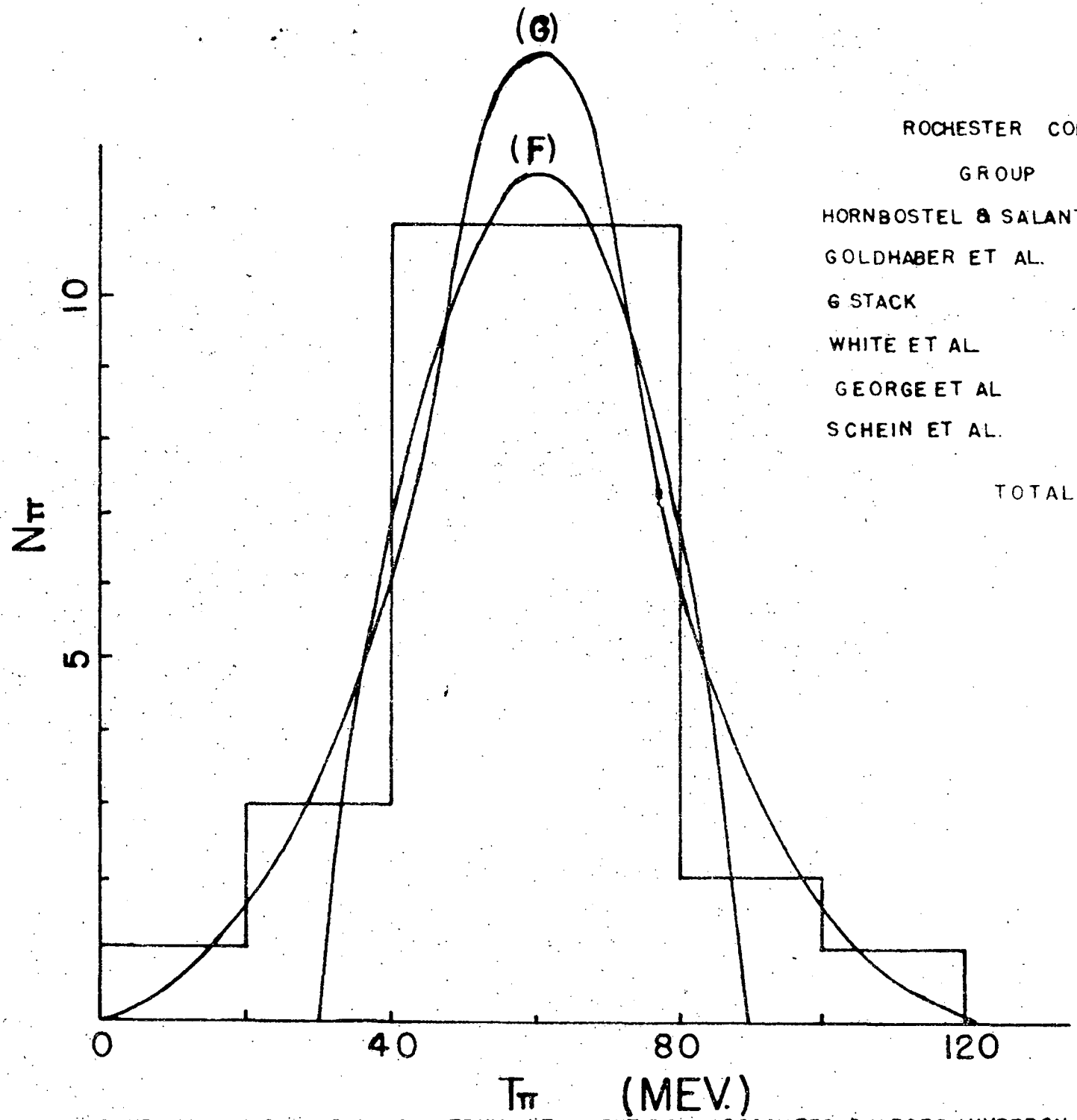

ROCHESTER COMPILATION

GROUP	NO. OF EVENTS K^-	$\pi^\pm_\Sigma$
HORNBOSTEL & SALANT	30	5
GOLDHABER ET AL.	138	5
G STACK	45	6
WHITE ET AL.	75	7
GEORGE ET AL	50	1
SCHEIN ET AL.	70	5
TOTAL	408	23

FIGURE 11. CHARGED PION SPECTRUM WITH IDENTIFIED ASSOCIATED CHARGED HYPERON

(G) USING GAUSSIAN DISTRIBUTION

(F) USING FERMI DISTRIBUTION

The calculated curve using the Fermi distribution has no tails due to the neglect of the high momentum components in the nucleus, and as is seen, does not fit the experimental data as well as the curve calculated using the Gaussian distribution.

2. Charged Pion Spectrum

This spectrum is the observed charged pion energy spectrum from all the K^- absorption stars in which a charged pion is observed to be emitted. The same uncertainties in the determination of the pion energies apply as previously described in Section G - 1.

Only a small fraction of the pions are observed to be emitted with energies above 100 Mev., which indicates that the frequency of the process is low ($K^- N^+ \rightarrow \Lambda \pi$). Even though the pion energy measurements in this region are not accurately determined, the observed fraction of pions emitted in this region, and considering the errors of the individual pion energy measurements, shows that the Λ° process probably does occus. A definite establishment of the Λ° process would be the observation of a charged pion with an accurately determined energy greater than ~ 130 Mev.

In the experimental histogram (Figure) there are 124 pions of which 11 have energies greater than 100 Mev. We have assumed that all the pions above 100 Mev. arose from the Λ° process.

From the calculated π^-_Λ elastic spectrum, (Figure), 71% of the emitted elastic pions have energies above 100 Mev.

The number of π^-_Λ elastic pions emitted will then be given by:

$$\frac{\text{No. } \pi^-_\Lambda \text{ elastic } (N_e)}{\text{No. of } \pi^-_\Lambda \text{ elastic with } T_\pi > 100 \text{ Mev.}} = \frac{N_e}{11 \text{ events}} = \frac{1.0}{.71}$$

The number of π^-_Λ elastic events is then $N_e = 15.5$ events.

We have calculated that the inelastic π_Λ^- contribution (Section) is equal to 35% of the elastic contribution or 26% of all the π_Λ^- mesons emitted. The number of inelastic π_Λ^- events is then given by:

$$\frac{\text{No. } \pi_\Lambda^- \text{ inelastic } (N_i(\pi_\Lambda^-))}{\text{No. } \pi_\Lambda^- \text{ elastic } (N_e(\pi_\Lambda^-))} = \frac{N_i(\pi_\Lambda^-)}{11} = \frac{.35}{.71}$$

The number of π^- inelastic events is then $N_i(\pi_\Lambda^-) = 5.5$ events.

The number of pions arising from the Λ^0 process in the histogram is then $N_{(\pi_\Lambda^-)} = N_e(\pi_\Lambda^-) + N_i(\pi_\Lambda^-) = 15.5 + 5.5 = 21$ events, and the number of charged pions arising from the Λ^0 process emitted below 100 Mev. is 21 - 11 = 10 events. This leaves 103 pions as the contribution of the Σ process.

We have calculated that 55% of the π_Λ^- pions originally formed within the nucleus are emitted composed of an elastic contribution of 41% of the original value and an inelastic contribution of 14% of the original value (Sect.). Similarly for the $\pi_\Sigma^\pm$ spectrum 70% of the originally formed $\pi_\Sigma^\pm$ pions are emitted from the nucleus where 68% of the original value are elastic and 2% are inelastic pions.

The ratio of emitted charged pions from the Λ^0 to the $\Sigma^{+,0,-}$ processes is

$$\frac{\pi_\Lambda^- \text{ emitted}}{\pi_\Sigma^\pm \text{ emitted}} = \frac{21}{103} = .20$$

The emission of pions due to the mesonic decay of a trapped or via the reaction $K^- \text{"}\eta\text{"} \rightarrow Y + \pi + \pi$ are small since no established case of two pion emission has been reported in approximately ~ 1000 K^- absorption stars so far reported.

The ratio of the amount of originally formed charged pions from the Λ^0 process $\pi(o)$ to the Σ process is then:

$$\frac{\pi_\Lambda^-(o)}{\pi_\Sigma^\pm(o)} = \frac{\%\text{ attenuation of } \pi_\Sigma^\pm}{\%\text{ attenuation of } \pi_\Lambda^-} \quad \frac{\pi_\Lambda^-(e)}{\pi^\pm(e)}$$

$$= \frac{.70}{.55} \quad \frac{21}{103}$$

$$\frac{\pi_\Lambda^-(o)}{\pi_\Sigma^\pm(o)} = .26 \pm .08$$ probable error on 11 events

From the branching ratios for the single nucleon K^- absorption process (Section) the ratio of the Λ^0 to Σ reactions is related to the ratio of the charged pions from the Λ^0 reaction to the charged pions from the Σ reaction ($\pi_\Lambda^- / \pi_\Sigma^+ + \pi_\Sigma^-$) by the equation:

$$\frac{\Lambda^0 / \Sigma^+ + \Sigma^0 + \Sigma^-}{\pi_\Lambda^- / \pi_\Sigma^+ + \pi_\Sigma^-} = \frac{(2\xi + 1)\ (3a^2 + 3\xi a^2 + 2b^2)}{6\xi\ (a^2 + 2\xi a^2 + b^2)}$$

where a and b are the intensity of the triplet and singlet Σ states respectively and ξ is the n/p ratio.

When the n/p is unity the ratio is

$$\frac{\Lambda^0 / \Sigma^+ + \Sigma^0 + \Sigma^-}{\pi_\Lambda^- / \pi_\Sigma^+ + \pi_\Sigma^-} = 1.$$

In emulsion the n/p ratio is 1.2, and for this case the expression becomes

$$\frac{\Lambda^0 / \Sigma^+ + \Sigma^0 + \Sigma^-}{\pi_\Lambda^- / \pi_\Sigma^+ + \pi_\Sigma^-} = \frac{1.7}{1.2}\left(\frac{1.1 + \frac{1}{3}\delta^2}{1.7 + \frac{1}{2}\delta^2}\right)$$

where $\delta^2 = b^2 / a^2$.

The ratio of δ^2 or b^2/a^2 is not well known but it is restricted to the range o to ∞ , which implies that the ratio $\frac{\Lambda^0 / \Sigma^+ + \Sigma^0 + \Sigma^-}{\pi_\Lambda^- / \pi_\Sigma^+ + \pi_\Sigma^-}$ can be between .917 and .945 for an n/p ratio of 1.2. We will use a

value of .93 and include the additional uncertainty in the statement of the probable error. The resulting ratio of K^- single nucleon nucleus processes which proceed through the Λ^0 mode to the Σ modes ($\Lambda^0/\Sigma^+ + \Sigma^0 + \Sigma^-$) is then:

$$\Lambda^0/\Sigma^+ + \Sigma^0 + \Sigma^- = .24 \pm .09$$

The calculated spectra for the emitted π_Λ^- and $\pi_\Sigma^\pm$ mesons (using the Gaussian distribution) normalized to the experimental histogram are given in Figure . The calculated elastic π_Λ^- spectrum was fitted to the experimental data by equating the area under the calculated curve above 100 Mev. to the area of the histogram above 100 Mev. The calculated amount and energy distribution of the emitted inelastic π_Λ^- pions were then added to this curve. The fitted contribution of emitted π_Λ^- pions was then subtracted from the histogram leaving the contribution of $\pi_\Sigma^\pm$ pions.

The calculated emitted $\pi_\Sigma^\pm$ spectrum was then fitted to the modified histogram by equating the area under the calculated curve in the region 20 - 80 Mev. to the area under the modified histogram in this energy interval.

Very good agreement is obtained between the calculated spectra and the experimental histogram.

Again using the branching ratio for the single nucleon absorption reactions (Sect.) the ratio of neutral pion to total pion production for the Σ and Λ process is given by:

$$\frac{\pi_\Sigma^0}{\pi_\Sigma^+ + \pi_\Sigma^0 + \pi_\Sigma^-} = \frac{\delta^2 + 3\xi}{3\delta^2 + 3 + 6\xi}$$

and $$\frac{\pi_\Lambda^0}{\pi_\Lambda^- + \pi_\Lambda^0} = \frac{1}{1+\xi}$$

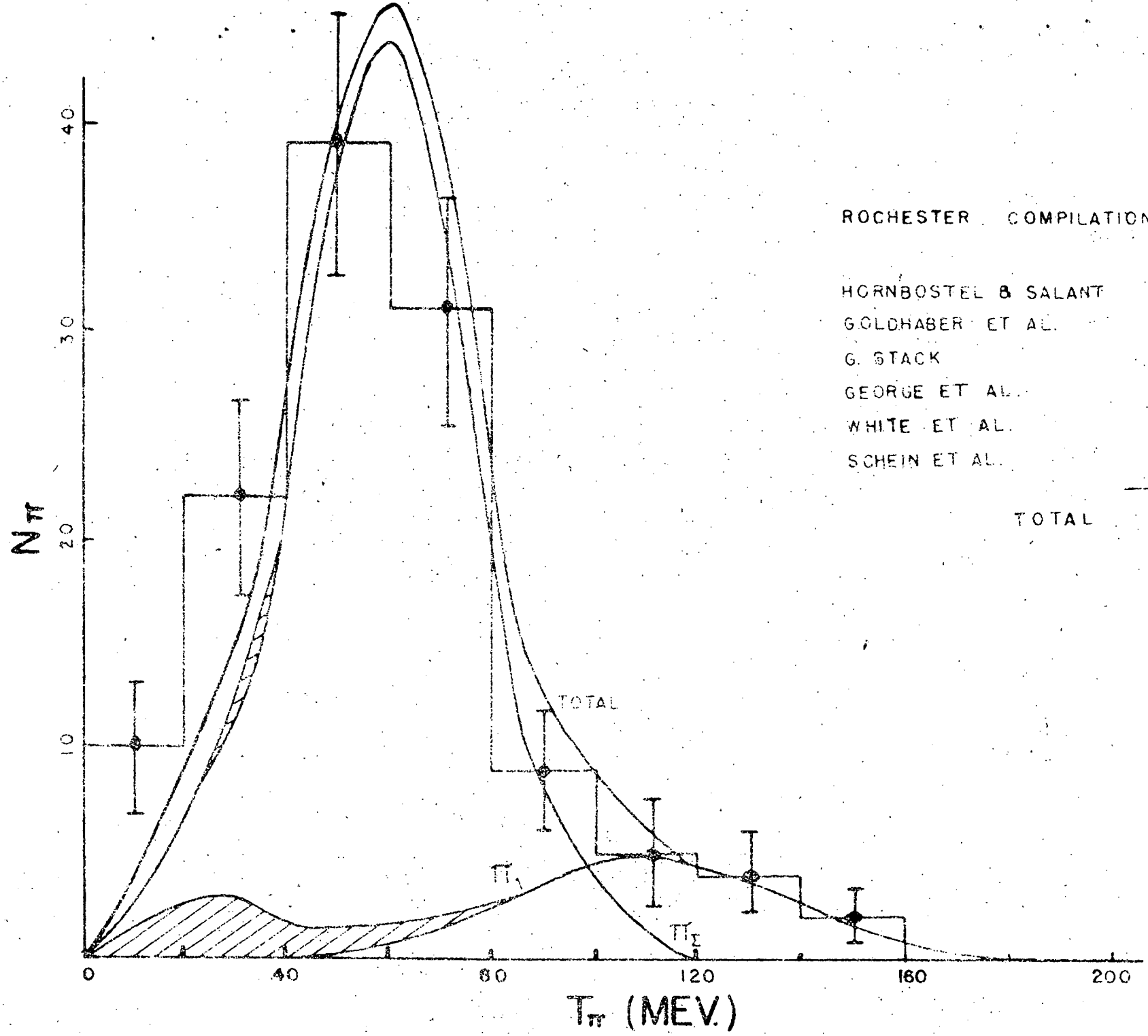

ROCHESTER COMPILATION

	K^-	π	$\Sigma\pi$
HORNBOSTEL & SALANT	30	15	5
GOLDHABER ET AL.	138	33	5
G. STACK	45	23	6
GEORGE ET AL.	52	10	1
WHITE ET AL.	75	23	7
SCHEIN ET AL.	70	20	5
TOTAL	410	124	29

FIGURE 12, OBSERVED & FITTED PION SPECTRA

For $n/p = \xi = 1$ these relations reduce to:

$$\frac{\pi_\Sigma^0}{\pi_\Sigma^{\pm,0}} = \frac{1}{3} \quad \text{and} \quad \frac{\pi_\Lambda^0}{\pi_\Lambda^{0,-}} = \frac{1}{2}$$

For the n/p ratio of the emulsion, i.e $\xi = n/p = 1.2$. These relations reduce to:

$$\frac{\pi_\Sigma^0}{\pi_\Sigma^{\pm,0}} = \frac{\delta^2 + 3.6}{10.2 + 3\delta^2} \quad \text{Can be between .33 to .35}$$

$$\text{and} \quad \frac{\pi_\Lambda^0}{\pi_\Lambda^{0,-}} = \frac{1}{2.2} = .45$$

We can now compare the observed frequency of charged pion emission with the amount which would be predicted by this analysis for various frequencies of the single nucleon process. This is done in Table VIII.

Using the branching ratios (Sect.) and normalizing the K^- p reaction to unity we obtain

$$\frac{a^2 + b^2 + c^2}{2} = 1$$

then a^2, b^2 and c^2 are each restricted to the range 0 to 2. The sum of the K^- p and K^- n reaction can then be written as

$$(K^- p + K^- n) = 1 + \xi (a^2 + b^2)$$

The ratio of the Λ^0 reactions to all the K^- "N" reactions in terms of the intensities

$$\frac{\Lambda^0}{(K^- \text{"N"})_{all}} = \frac{3/2 \; c^2}{1 + \xi (a^2 + c^2)}$$

$$= .19 \pm .08 \quad \text{(experimental value)}$$

Equations relating the intensities can be written for $\xi = 1.2$.

$$c^2 = .15 \pm .08 + (.18 \pm .09)\, a^2$$

c^2 is then restricted to the range:

TABLE VIII

Frequencies of Pion Production

	This Analysis (n/p = 1.2)		Observed Frequency %
Single Nucleon Frequency 100%	Frequency at Production %	Emitted Frequency %	
Σ reactions			
	81 ± 7		(25)
$\pi_\Sigma^+ + \pi_\Sigma^-$	52 ± 5 to 54 ± 5	36 ± 4 to 38 ± 4	
Λ reactions	19 ± 7		(5)
π_Λ^-	10 ± 4	5 ± 2	
		42 ± 5	31 ± 4%
Total			
Single Nucleon Frequency 90%			
Σ reactions	73 ± 6		
$\pi_\Sigma^+ + \pi_\Sigma^-$	47 ± 5	33 ± 4	
Λ reactions	17 ± 6		
π_Λ^-	9 ± 4	4 ± 2	
Total		37 ± 5	31 ± 4

$$c^2 = .15 \pm .08 \quad \text{if } a^2 = 0$$
$$c^2 = .41 \pm .11 \quad \text{if } a^2 = 2$$

Furthermore, it can easily be seen that if the value of c^2 is in the lower part of this range most of the Σ formation proceeds through the singlet state (b^2 large, a^2 small), and if the value of c^2 is in the high part of this range most of the Σ formation proceeds through the triplet state (a^2 large, b^2 small).

3. Charged Hyperon Spectrum

The observed and calculated spectra (using the Gaussien momentum distribution and normalized to the data above 10 Mev) are compared in figure 14.

It is seen that they agree very well above 10 Mev. from the sparcity of events above 60 Mev, the two nucleon process is indicated to have a low frequency of occurrence. The two nucleon process ($K^- + "N" + "N"$ $Y + N$) would yield a high energy hyperon of 110 ± 60 Mev. Although some of the high energy hyperons could have remained undetected due to the small sizes of the stacks employed. Of the particles of nucleonic mass (considering only our data) emitted with kinetic energies greater than 50 Mev, twelve were arrested in the emulsion of which one was an identified Σ^+ and twelve left the stacks (lifetime considerations make the decay in flight of many of the high energy hyperons very likely). From these considerations and the calculated fit the two nucleon process is infrequent although it is difficult to estimate its frequency due to isotopic spin, and some experimental considerations, but it is probably $< 10\%$.

There is evidence for a Coulomb barrier effect inhibiting the emission of low energy positive hyperons. In Table IX are displayed the frequency of Σ^- and Σ^+ hyperon emission for 10 Mev energy intervals for the events in which the charge has been reported.

Table IX

Energy Interval	0 - 10,	10 - 20,	20 - 30,	30 - 40 Mev
	7	3	2	2
	2 + (1)	5	3	1

The ratios are: $\Sigma^-/\Sigma^+ (< 10 \text{ Mev}) = \frac{7}{2 + (1)}$; $\Sigma^-/\Sigma^+ (> 10 \text{ Mev}) = \frac{7}{9}$

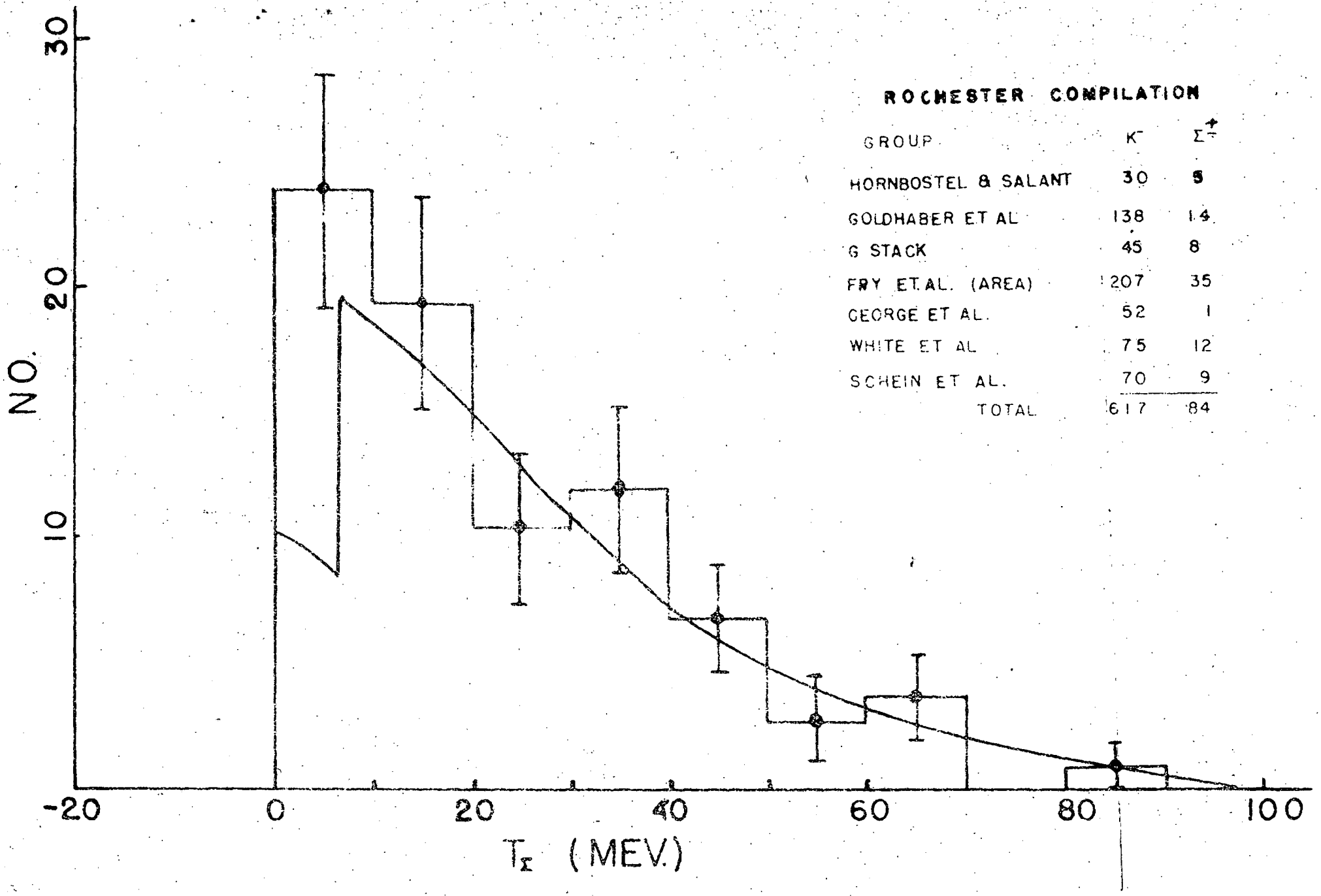

FIGURE 13, HYPERON KINETIC ENERGY SPECTRUM

The hyperon spectra were fitted to the experimental hi s-togram by using a Σ^-/Σ^+ detected emission of unity and then averaging the calculated Σ^- and Σ^+ spectra, and fitting this final curve to the data. The Σ^- and Σ^+ hyperon spectra included the Coulomb shifts. Eventhough many of the Σ hyperons remain undected, they have no influence on this fitting procedure.

4. Sum of Kinetic Energies of Σ Hyperon and its Associated Charged Pion

In Figure 14 is shown the sum of the observed kinetic energies of the Σ hyperon and its associated charged pion ($\sigma_{\Sigma\pi}$ events).

The energy conservation equation can be expressed in terms of the sum of the kinetic energies of the Σ hyperon and its associated charged pion (where neither particle has suffered an inelastic scattering in leaving the nucleus).

$$T_{\pi} + T_{\Sigma} = M_p + M_{K^-} - M_{\Sigma} - M_{\pi} + BE_{a,K^-} + B_N$$

Using the Σ^-, Σ^+ mass values from Part II, a value of -8 Mev. as the K^- atomic binding and B_N as the binding energy of the nucleon with which the K^- interacts the equations become:

$$T_{\pi^-} + T_{\Sigma^+} = 103 - 8 + B_N = 95 \text{ Mev} + B_N \quad \text{(for } \Sigma^+\pi^- \text{ reactions)}$$

$$T_{\pi^+} + T_{\Sigma^-} = 96 - 8 + B_N = 88 \text{ Mev} + B_N \quad \text{(for } \Sigma^-\pi^+ \text{ reactions)}$$

For comparison the K^- free nucleon energies are

$$T_{\pi^-} + T_{\Sigma^+} = 103$$

$$T_{\pi^+} + T_{\Sigma^-} = 96 \text{ Mev}$$

The sum of kinetic energies in the K^- nucleon nucleus will vary between

$T_{\pi^-} + T_{\Sigma^+}$ from 53 to 87 Mev. and

$T_{\pi^+} + T_{\Sigma^-}$ from 45 to 80 Mev.

For the variation of B_N from -8 Mev to 42 Mev.

The average sum of the kinetic energies will be

$\overline{T_{\pi^\mp}} + \overline{T_{\Sigma^\pm}} = 70$ Mev. for equal production of Σ^+ and Σ^- hyperons which corresponds to a residual nuclear excitation of 13 Mev.

The observed average sum of energies is: $\overline{T_{\pi^\mp}} + \overline{T_{\Sigma^\pm}} = 75$ Mev. (excluding the low energy event in the histogram) which is in agreement with the single nucleon interpretation.

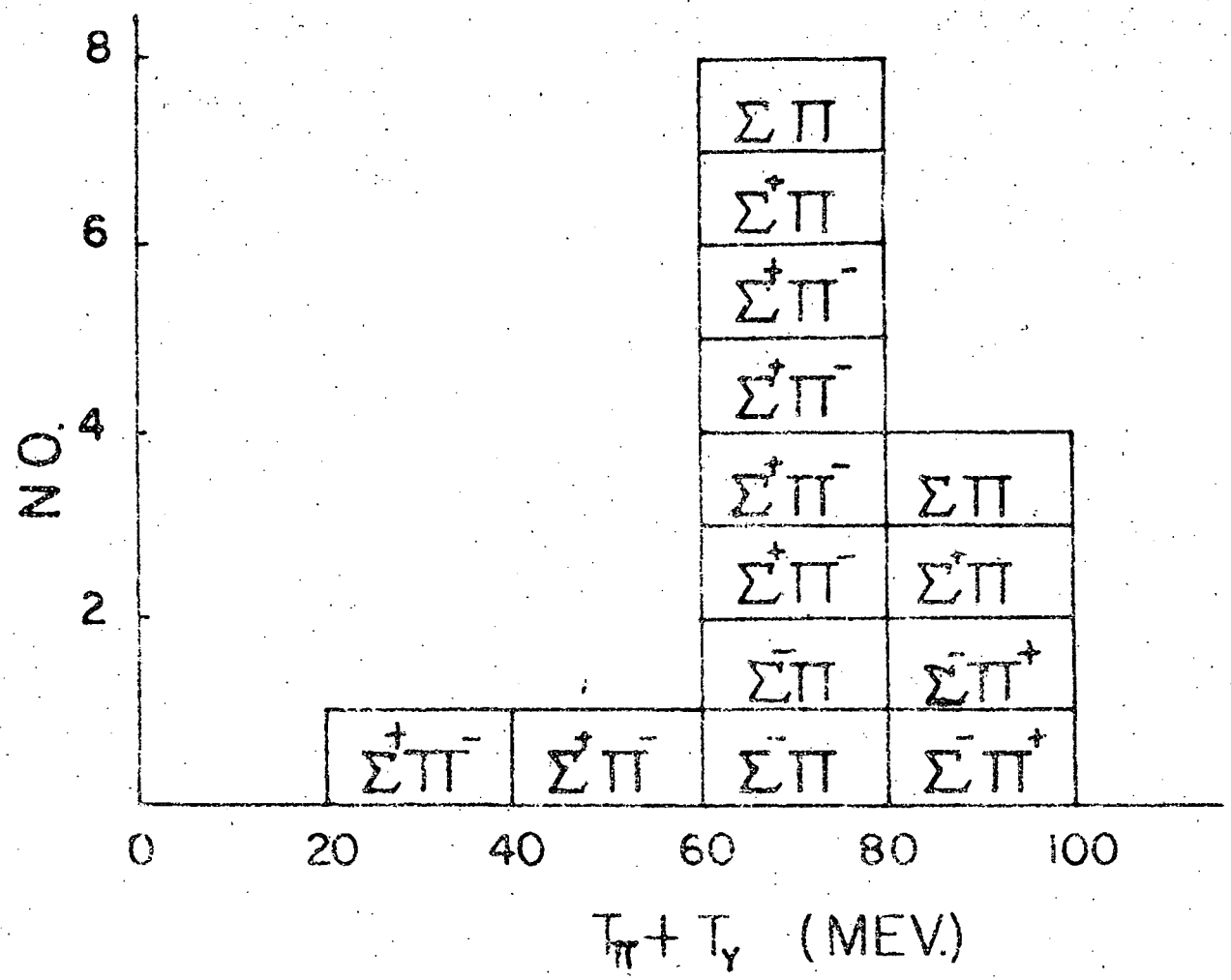

ROCHESTER COMPILATION

GROUP	NUMBER OF EVENTS
HORNBOSTEL & SALANT	2
FRY ET AL.	1
GOLDHABER ET AL.	3
GEORGE ET AL.	1
WHITE ET AL.	5
SCHEIN ET AL.	1
LEPRINCE-RINGUET ET AL	1
TOTAL	14

FIGURE 14. SUM OF KINETIC ENERGIES OF ASSOCIATED Σ AND π

5. Division of Energy Released

An estimate of the division of energy among the particles emitted from an average K^- absorption star can be made.

The average energy emitted in knock-on nucleons, $\bar{U}_{ko}$, can be obtained by assuming that knock-on neutrons have the same average energy as knock-on protons whose average energy is obtained from the fast proton spectrum. The n/p ratio was taken as:

$$\langle n/p \rangle = \left\langle \frac{A - Z}{Z} \right\rangle_{emul.} = 1.2$$

The average energy released in evaporation processes, $\bar{U}_{ev}$, has been obtained by computing the average energy released in slow protons*. The average energy released in evaporation neutrons was obtained by using a value of 3 Mev. for the average kinetic energy of evaporation neutrons[24] ($\bar{E}_n = \bar{T}_n + B.E. \approx 11$ Mev.) and a n/p ratio of 4 [24].

The average energy emitted in charged unstable particles has been obtained by adding a correction term to the number of emitted charged hyperons and pions to account for those which remain undetected, we increased the number of pions by 10% and the number of Σ^- hyperons by 100% and used the observed average energies.

The average energy emitted in π^0 and Σ^0 particles was estimated on the basis of charge independence and by assuming that the interaction properties of the π^0 are the same as the $\pi^\pm$, and that Σ^0 hyperon has the same interaction properties as the $\Sigma^\pm$ hyperons.

---

* For the evaporation region we have assumed the same α/p ratio and energy spectra for the α's and protons as has been observed in π^- meson absorption stars.[25]

Table XI

Division of Energy Released in an Average K^- Star

Emission in:		Energy in Mev.	Data
Evaporation Processes	$\bar{U}_{ev.}$	77	(Goldhaber et. al.)
Knock-on Nucleons	$\bar{U}_{ko}$	62	(Goldhaber et. al.)
Charged Pions	$\bar{U}_{\pi^\pm}$	67	(Rochester compilatiion)
Charged Hyperons	$\bar{U}_{\Sigma^\pm}$	58	(Rochester compilation)
Hyperfragments	$\bar{U}_{Hyper.}$	5	(Goldhaber et.al.)
Neutral Pions	$\bar{U}_{\pi^0}$	33	(charge independence)
Neutral Σ^0 Hyperons	$\bar{U}_{\Sigma^0}$	29	(charge independence)
Energy accounted for	$\bar{U}$	331 Mev.	

The small average energy emitted in hyperfragments is also included. The resulting energies are given in Table XI.

The total energy available, $E_{avil.}$, in the K^- - nucleon absorption in complex nuclei is:

$$E_{avil.} = M_{K^-} c^2 - B.E._{a,K^-} - B.E._{last\ nucleon}$$

$$= (493 - 8 - 8)\ \text{Mev.} = 477\ \text{Mev.}$$

The average energy given off in unstable neutral particles is from Table XI :

$$E_{\substack{unstable \\ neutral\ particles}} = (477 - 269)\ \text{Mev.} = 208\ \text{Mev.}$$

Including the energy estimated to be carried away by Σ^0 and π^0 particles we obtain:

$$E_{extra} = 146\ \text{Mev.}$$

This unaccounted amount of energy would be carried away by emitted Λ^0 particles. The Λ^0 particles arise from two sources, the primary process $K^- N \rightarrow \Lambda^0 \pi$ and from the secondary interactions of the hyperons by $\Sigma N \sim \Lambda^0 N$; both of these processes will emit Λ^0 particles with an average kinetic energy of about 40 Mev.

The fraction of K^- stars in which a Λ^0 particle is emitted is given by:

$$\frac{E_{extra}}{M_K c^2 - M_p c^2 + K.E.} = \frac{146}{217} = 67\ \%.$$

This fraction can also be obtained by considering the conservation of strangeness.

We determine the percentage of stars in which the strangeness is visably accounted for and interprete the missing strangeness as being carried away by emitted Λ^0 particles. The results are given in Table XII.

Table XII

Percentage of K^- Stars in which Strangeness is Visably Accounted for.

	% Emitted	
$\Sigma^{\pm}$ obs	14	observed
Σ^- missed	7	estimated
Σ^0	10	charge independence
Hyperfragments	3	observed
Stars in which total visible energy is greater than 310 Mev. & no strange particle observed.	1	observed
Total strangeness accounted for:	35%	

This method yields 65 % of the K^- absorption stars will emit Λ^0 particles.

APPENDIX

In this section we will discuss the approximations made in treating the $K^- N \rightarrow Y\pi$ reactions inside the nucleus.

In section the energ conservation equation was written:

$$E_i = E_f$$

where: $E_i = M_N + M_K + B_N + B.E._{a,K^-}$

and $E_f = M_Y + M_\pi + T_Y + T_\pi$.

The various symbols were previously defined in section .

Using the transformations from outside the nucleus to inside the nucleus

$$T_\pi = T_{\pi i} + V_\pi$$

$$T_Y = T_{Y i} + V_Y$$

$$B_N = T_{Ni} + V_N ,$$

we can rewrite the energy conservation equation,

$$E_I = T_{\pi i} + T_{Yi} + M_Y + M_\pi = T_{Ni} + V_N - V_\pi - V_Y + B.E._{a,K^-} + M_N + M_K .$$

We write the momentum conservation equation as (assuming the $\vec{p_K} = 0$)

$$\vec{p_{Ni}} = \vec{p_{\pi i}} + \vec{p_{Yi}} .$$

The energy available in the center of mass system is

$$E_{cm.} = \sqrt{E_I^2 - p_{Ni}^2}$$

Rewriting $E_I = M_N + T_{Ni} + A$, where $A = V_N + B.E._{a,K^-} - V_Y - V_\pi + M_K$ and using $p_{Ni}^2 = T_{Ni} (T_{Ni} + 2M_N)$ then

$$E_{cm} = (A + M_N) \sqrt{1 + \frac{2AT_{Ni}}{(A + M_N)^2}}$$

Using the values given in section

$$A = (-42 + 40 + 15 - 8 + 494) \text{ Mev.} = 499 \text{ Mev.}$$

and $M_N = 938$ Mev. then $2A/(A + M_N) = .696$.

For $T_{N1} = 40$ Mev. the term $2A\,T_N/(A + M_N)^2$ is small compared to one, we can now approximate E_{cm} by

$$E_{cm} = (A + M_N)\left(1 + \frac{A\,T_N}{(A + M_N)^2}\right)$$

$$= E_o + \Delta$$

where $E_o = A + M_N$, and $\Delta = A\,T_N/(A + M_N)$.

Substituting

$$E_{cm} = 1437 \text{ Mev.} + .348\,T_{N1}.$$

The effect of variations of the nucleon kinectic energy, T_{N1}, from 0- 40 Mev. on the energy in the center of mass, E_{cm}, is small.

The momentum in the center of mass, p_{cm}, is given by

$$p_{cm} = \frac{1}{2E_{cm}}\sqrt{(E_{cm}^2 - (M_Y + M)^2)(E_{cm}^2 - (M_Y - M)^2)}$$

Letting $a^2 = (M_Y + M)^2$ and $b^2 = (M_Y - M)^2$ and approximating $E_{cm}^2 = E_o^2 + 2E_o\Delta$ then

$$p_{cm} = \frac{1}{2(E_o + \Delta)}\sqrt{(E_o^2 + 2E_o - a^2)(E_o^2 + 2E_o - b^2)}$$

and

$$p_o = \frac{1}{2E_o}\sqrt{(E_o^2 - a^2)(E_o^2 - b^2)}$$

carrying out the indicated operations and neglecting second order terms

$$p_{cm} = p_o\left(1 + \frac{\Delta}{E_o}\left(\frac{E_o^2}{E_o^2 - b^2} + \frac{E_o^2}{E_o^2 - a^2} - 1\right)\right)$$

For the $\Sigma\pi$ reaction

$$p_o = 187 \frac{Mev}{c} \quad , \quad T_\Sigma = 14.6 \text{ Mev} \quad , \quad T_\pi = 93 \text{ Mev}$$

$$p_{cm} = p_o \quad (1 + 1.972 \times 10^{-3} \; T_{N_1})$$

For the $\Lambda\pi$ reaction

$$p\,o = 257 \frac{Mev}{c} \quad , \quad T_\Lambda = 29.3 \text{ Mev} \quad , \quad T_\pi = 153 \text{ Mev}$$

$$p_{cm} = p\,o \quad (1 + 1.232 \times 10^{-3} \; T_{N_1})$$

The momentum in the center of mass, p_{cm} changes at most by 7% for variations of T_{N_1} from 0 to 40 Mev. In the calculations in Section we have neglected this variation and used a constant value of p_{cm} (for T_{N_1} = 20 Mev).

REFERENCES

1. Leprince Ringuet, Fong, Janneau, and Morellet, Comp. rend: 226, 1897 (1948); Leprince Ringuet, Rev. Mod. Phy: 21, 42 (1949).

2. D. Lal, Y. Pal, and B. Peters, Proc. Indian Aca. of Sci.: XXXVIII, 398 (1953); W. F. Fry, and J. J. Lord, Phys. Rev.: 92, 438 (1953); Di Corato, Locatelli, Mignone, and Tomasini, Nuovo cimento, 12, Supp. 2 270 (1954); H. DeStaebler, Phys. Rev. 95, 1110 (1954); J. Hornbostel, and E. O. Salent, Phys. Rev. 93, 902 (1954); Naugle, Ney, Frier, and Cheston, Phys. Rev., 96, 1383 (1954); Boggild, Hooper, and Scharff, Nuovo cimento, 12, Suppl 2, 273 (1954); MacPherson, Major, Parbash, Rochester, and Short, Nuovo cimento, 12, Suppl 2, 275 (1954); S. von Friesen, Nuovo cimento, 12, Suppl. 2, 273 (1954); Arkiv Fisik, 8, 305 (1954).

3. M. Gell-Mann, and A. Pais, Proc. of Glasgow Conf. (Pergamon Press, London, 1955); M. Gell-Mann, Phys. Rev., 92, 833, (1953); Pisa Conference, Nuovo cimento, to be published (1955); T. Nakano, and K. Nishijima, Progr. of Theoret. Phys. (Japan) 10, 581 (1954); M. Goldhaber, Phys. Rev., 101, 433 (1956); R. G. Sacks, Phys. Rev. 99, 1576 (1955); Friedlander, Fujimoto, Keefe, and Menon, Nuovo cimento, 2, 90 (1955).

4. J. Hornbostel, and E. O. Salant, Phys. Rev. 98, 218 (1955), 102, 502 (1956); S. C. Freden, and H. K. Ticho, Phys. Sev. 99, 1057 (1955); Fry, Schneps, Snow, and Swami, Phys. Rev., 100, 950, 1448 (1955); Chupp, Goldhaber, Goldhaber, and Webb, Proc. of Pisa Conf, 1955 to be published in Nuovo Cimento and U. C. R. L. 3044 (unpublished) 1955; G. Stack Collaborators, Proc. of Pisa Conf. 1955, to be published in Nuovo cimento; George, Hers, Noon, and Solntseff, Nuovo cimento, 10, 95 (1956); Haskin, Bowen, and Schein, Phys. Rev. 103, 1512 (1956); S. Goldhaber, Proc. of

Reprinted from THE PHYSICAL REVIEW, Vol. 101, No. 3, 1212–1214, February 1, 1956
Printed in U. S. A.

II. The K^- Mass, Σ^- Mass and $\Sigma^- - \Sigma^+$ Mass Difference

RADIATION LABORATORY
REPRINT NUMBER
1956 5 2
UNIVERSITY OF CALIFORNIA

A. Ratio of K^- Mass to K^+ Mass*

FRANCIS H. WEBB, WARREN W. CHUPP, GERSON GOLDHABER, AND SULAMITH GOLDHABER
Radiation Laboratory, University of California, Berkeley, California

(Received December 14, 1955)

MEASUREMENTS on the mass of the positive K particle have recently been carried out by direct comparison of the ranges of K^+ and τ^+ mesons and by comparison of ranges of K^+ mesons and protons of the same momentum.[1–4] For negative K particles no such direct comparison is possible. Hornbostel and Salant[5] determined the K^- mass by a range-momentum method as $931 \pm 24\ m_e$.

In order to compare the negative K-meson mass with the positive K-meson mass, we have exposed stacks of nuclear emulsions to the focused K^+ and K^- beams[1,2] of the Bevatron, maintaining the geometry constant and reversing the magnetic field[6] in the focusing spectrometer.

The stacks were exposed with the plane of the emulsions in the vertical direction. The horizontal momentum dispersion in the analyzing magnet gives rise to a momentum spread across the stacks. The momentum in the K^+ stack (forty 600-μ Ilford G.5 pellicles) varies from about 315 Mev/c to 335 Mev/c, and that of the K^- stacks (one hundred and thirty-two 600-μ pellicles) from about 280 Mev/c to 355 Mev/c. Immediately behind the stacks, a copper absorber and wedge were placed to stop the positive and negative π mesons in the respective exposures. The geometry of the exposure is shown in Fig. 1.

The scanning method used in this experiment was

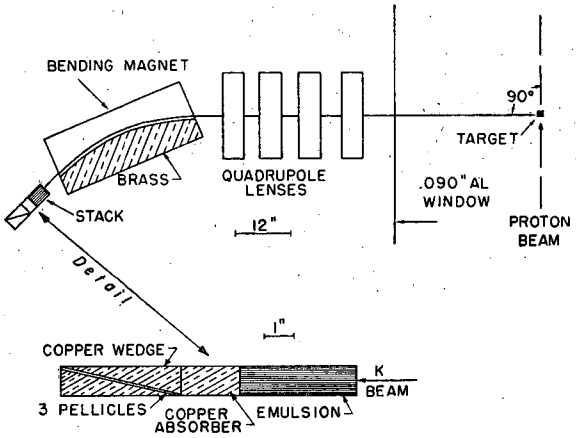

FIG. 1. Exposure geometry.

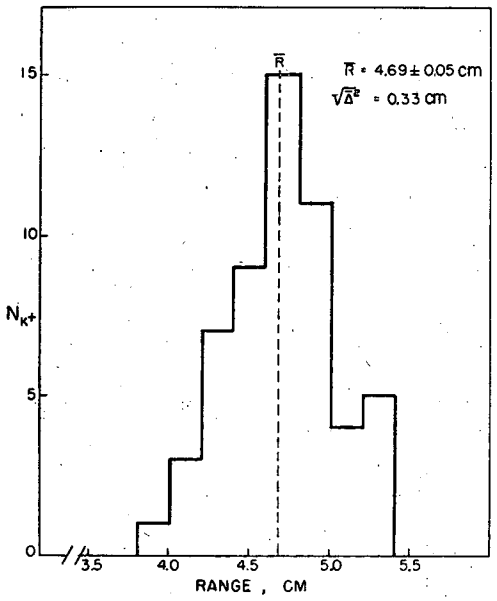

FIG. 2. Range distribution of positive K mesons.

"scanning along the track." Tracks were picked on the basis of their ionization (grain density) at the entering edge of the emulsion in the negative stack and 1 cm from the edge (i.e., after the region in which the protons of the same momentum stop) in the positive stack. The limits of the grain density at which a particle was selected were chosen so as to include particles between the mass of 700 m_e and 1300 m_e. All K mesons that underwent a nuclear scattering (scattering $>20°$ for $E_K > 30$ Mev) were eliminated from the sample chosen for the K^--mass determination. Three K^- mesons and two K^+ mesons were eliminated in this fashion. The method employed for the K^--mass determination was as follows:

1. The ranges of the positive K mesons were used to determine the momentum of the positive channel. The mass of the K^+ used for the momentum determination is $M_{K^+} = M_\tau = 965.4\ m_e$. It should be noted that the M_{K^-}/M_{K^+} ratio is not sensitive to this assumption. Figure 2 shows the range distribution of the positive K mesons.

2. Both the positive and negative π mesons were stopped with a copper absorber and wedge (under the same geometry), permitting us to determine the π^+ and π^- range difference. This was accomplished by observation of stopping π mesons in pellicles placed in the wedge. The knowledge of the momentum in the positive channel and of the difference in the π^+ and π^- ranges permits us to calculate the momentum in the negative channel. This calculation was carried out by integrating the function dp/dR, by use of Aron's tables.[7] The difference in the momenta obtained from the pion range difference ($R_{\pi^+}-R_{\pi^-}=1.46$ cm in emulsion) is 9 Mev/c. This method is not affected by the over-all accuracy to which the range-energy relation is known since it uses dE/dx to bridge across only a small momentum difference. The range distribution of the positive and negative π mesons is shown in Fig. 3.

3. The range of the negative K mesons, and the momentum in the negative channel obtained by Method 2, permitted us to determine the K^- mass.[8]

For the K^--mass determination we used the ranges of 42 K^- mesons found in the central part of the stack. Any error in the mass due to the error in the measurement of the momentum dispersion is thus negligible. The momentum dispersion was measured by wire trajectories[1] and checked by us with the range of protons in the positive channel. The uncertainties that contribute to the error in the K^- mass are (a) statistical errors; (b) alignment errors, which are of the same order

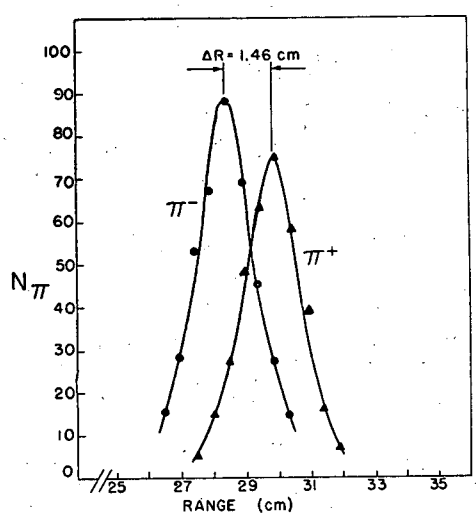

FIG. 3. Range distribution of positive and negative pions. The mesons traversed the stack and the copper absorber and wedge. The equivalent emulsion range is given by ρ emulsion$=3.85$ g/cm^2.

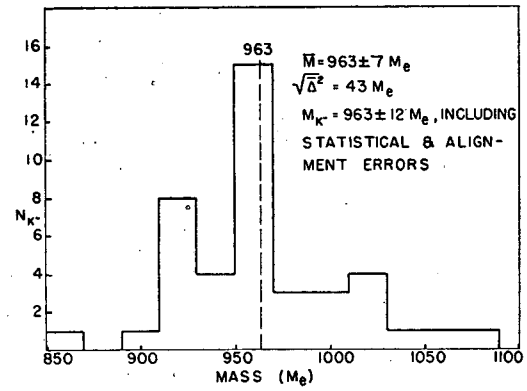

FIG. 4. Mass histogram of the negative K mesons (assuming $M_{K^+}=M_{\tau^+}=965.4\ m_e$).

as the statistical errors; (c) errors in range measurements, which are negligible compared with (a) and (b). As all our measurements were carried out relative to the K^+ range, systematic errors would tend to cancel. A mass histogram for these 42 mesons is shown in Fig. 4.

The ratio of the negative K-meson mass to positive K-meson mass thus obtained is

$$M_{K^-}/M_{K^+}=0.998\pm0.013.$$

The mass of the K^-, if we assume $M_{K^+}=M_\tau=965.4\ m_e$, is

$$M_{K^-}=963\pm12\ m_e.$$

The above mass determination corresponds to the mass of K mesons present, after a time of flight of 1.4×10^{-8} sec in the proper system of the K mesons.

We are greatly indebted to Dr. E. J. Lofgren and the Bevatron crew for their assistance in carrying out the exposures. We also wish to thank Mr. H. H. Bayona, G. M. Wike, and Mrs. C. Toche for their help in scanning the emulsions.

* This work was done under the auspices of the U. S. Atomic Energy Commission.

[1] Birge, Haddock, Kerth, Peterson, Sandweiss, Stork, and Whitehead, Phys. Rev. **99**, 329 (1955).
[2] Birge, Peterson, Stork, and Whitehead, Phys. Rev. **100**, 430 (1955).
[3] Fung, Pevsner, and Ritson (to be published).
[4] Heckman, Smith, and Barkas, University of California Radiation Laboratory Report No. UCRL-3156, 1955 (unpublished).
[5] J. Hornbostel and E. O. Salant, Phys. Rev. **99**, 338 (1955).
[6] The stray field of the Bevatron increases the magnetic field of the strong-focusing spectrometer for exposures to positive particles and decreases it for exposures to negative particles. A compensation for the stray field was made which almost cancelled this effect.
[7] Aron, Hoffman, and Williams, University of California Radiation Laboratory Report No. UCRL-121, 1949 (unpublished).
[8] Range-energy tables of W. H. Barkas and G. Hahn [University of California Radiation Laboratory Report No. UCRL-2579 (unpublished)] were used in this work.

Sixth Annual Rochester Conf. 1956, VI 1-10, Interscience (1956).

5. Kerth, Stork, Haddock, and Whitehead, Phys. Rev., 99, 641A (1955).

6. G. Goldhaber, S. Goldhaber, S. Goldsack, and J. Lannutti, UCRL-2928 (1955) unpublished.

7. Stiller, Shapiro, and O'Dell, Rev. Sci. Inst., 25, 340 (1954).

8. W. Barkas, UCRL-3384 (April, 1956) unpublished.

9. Private communication from Dr. Stork.

10. F. Webb, W. Chupp, G. Goldhaber, and S. Goldhaber, Phys. Rev., 101, 1212 (1956).

11. W. Barkas, and D. Young, UCRL-2579 (Sept., 1954) unpublished.

12. E. Iloff, G. Goldhaber, S. Goldhaber, J. Lannutti, C. Gilbert, C. Violet, S. White, Fournet, A. Pevsner, D. Ritson, and M. Widgoff, Phys. Rev. 102, 927 (1955).

13. Antiproton Collaboration Experiment, to be published in Phys. Rev., and UCRL-3520 (Sept., 1956) unpublished.

14. R. Serber, Phys. Rev. 72, 114 (1947); Ferretti, Gassaroli, and Stantic, Prog. Report No. 1, Physics Dept. University of Bologna, 1956, private communication from G. Puppi.

15. M. Koshiba, Nuovo cimento, 2, 357 (1956); D. Feldmann, UCRL-3168 (1955) unpublished; S. Gasiorowicz, UCRL-3074 (July, 1955) unpublished.

16. Camac, Halbert, and Platt, Phys. Rev., 99, 905 (1955); Camac, McGuire, Platt, and Schulte, Phys. Rev. 99, 897 (1955).

17. Blatt and Butler, Nuovo cimento, 2, 409 (1956); R. Serber, Phys. Rev. 72, 114 (1947); Francis, and Watson, Am. Jour. Phys. 21, 659, (1953).

18. The following values of the potentials were used:

V_n = - 42 Mev. real part of potential deduced by Feshbach, Porter, and Weisskopf, Phys. Rev., 96, 448 (1954).

V = - 40 Mev. approx. average value of real part of pion potential in energy region 40 to 150 Mev., Frank, Gammel, and Watson, Phys. Rev. 101, 891 (1956).

V_Y = - 15 Mev. (assumed value)

19. J. Blaton, On a Geometrical Interpretation of Energy and Momentum Conservation in Atomic Collisions and Disintegration Processes, Det. Kgl. Danske Vedenskabernes Selskab, Matematisk-Kysiske Meddelser, Bind XXIV, Nr. 20 (1950).

20. Brueckner, Serber, and Watson, Phys. Rev. 84, 258 (1951).

21. Frank, Gammel, and Watson, Phys. Rev. 101, 891 (1956).

22. Bernardini, Booth, and Lederman, Phys. Rev., 83, 1075 (1951); Bernardini, Booth, and Lederman, Phys. Rev., 83, 1277 (1951); Bernardini, and Levy, Phys. Rev., 84, 610 (1951); G. Goldhaber, and S. Goldhaber, Phys. Rev., 91, 467 (1953); and Proc. of Sixth Annual Rochester Conf. 1956, VI 1-10, Interscience, (1956); A. H. Morrish, Phys. Rev., 90, 674 (1953).

23. S. Goldhaber, Proc. of Sixth Annual Rochester Conf. 1956, VI 1-10, Interscience (1956).

24. E. E. Gross, UCRL-3330 (Feb., 1956) thesis, unpublished.

25. Menon, Muirhead, and Rochat, Phil. Mag. 41, 583 (1950).

B. The K^-, Σ^- Masses and the $\Sigma^- - \Sigma^+$ Mass Difference.

During the course of this study a type of event has been observed which deserves special attention.

Two events ($\sigma_{\pi\Sigma 1}$ and $\sigma_{\pi\Sigma 2}$) and two additional events observed at M.I.T. and Harvard (K_{MH1} and K_{MH2}) are of this type.

In each event a K^- meson is arrested in the emulsion and forms a visible absorption star composed of two prongs (no recoils, blobs, or electrons were associated with the star). One prong is a shower particle (presumably a π meson) which leaves the stack, and the other prong is a dark track several hundred microns long (of nucleonic mass) which is emitted colinear (within the precision of measurement) to the shower particle. In two of the events ($\sigma_{\pi\Sigma 1}$ and K_{MH1}) a minimum particle (presumably a π meson) is associated with the ending of the dark prong, indicating that the dark prong is either a Σ^+ particle which decayed at rest, or a $\Sigma^\pm$ particle which decayed in flight. In the other two events ($\sigma_{\pi\Sigma 2}$ and K_{MH2}) no visible secondary or interaction was formed at the end of the dark prong, which is consistant with a hyperon which is arrested in the emulsion forming a zero prong star.

Measurements on these four events are given in Table I.

These events are interpreted as the absorption at rest of the K^- meson by hydrogen in the emulsion by the following reactions:

$$K^- + H \longrightarrow \Sigma^\pm + \pi^\mp$$

Table I

Measurements on Colinear* Events

Event	Dark Prong (Σ)				Shower Particle (π)	
	Range	Dip z/100	Moderation Time in 10^{-11} sec.	at end	g/g_0	Dip z/100
$\sigma_\pi \Sigma_1$	809 ± 40	-41.4	2.5	minimum secondary	1.1 ± .2	+ 41.3
K_{MH1}	579 ± 25		2.0	minimum secondary	1.31 ± .7	
$\sigma_\pi \Sigma_2$	695 ± 25	+ 24.3	2.3	no visible secondary or interaction		-24.5
K_{MH2}	691 ± 45		2.3	no visible secondary or interaction		

* The projected colinearity of the dark prong and shower particle in all four events is better than $\frac{1}{2}^\circ$.

The mass of one of the particles in the foregoing reaction can be determined by using the measured range of the dark prong, the range-energy relation[1], the masses of the other three particles, and the conservation of energy and momentum.

A. The K^- Mass from the Σ^+ Mass.

We carried through the above procedure and determined the K^- mass for the two events ($\sigma_{\pi\Sigma 1}$ and K_{MH1}) where the dark prong is interpreted as a Σ^+ particle.

We used the following masses for the Σ^+ a value of $M_{\Sigma^+} = 2327 \pm 3\ m_e$[2] a π^- mass of $M_{\pi^-} = 272.7 \pm .3\ m_e$[3], and a proton mass of $M_p = 938.73$ Mev.[4] Since we were unable to determine if the hyperons reached their total potential range before decaying (due to their large dip) ;the K^- masses determined by this analysis are to be considered as lower limits to the K^- mass.

If the hyperon in event K_{MH1} decayed in flight the results would be more consistant. The total moderation time of the hyperons in these two events is 5.5×10^{-11} sec. and since the Σ^+ lifetime is $9 \pm 2 \times 10^{-11}$ sec.[5] the decay in flight of the hyperon in event K_{MH1} is reasonable.

If we apply the same procedure to the two Σ^- events and use a Σ^- mass equal to the Σ^+ mass and a π^+ mass equal to the π^- mass we obtain values of the K^- mass, on the basis of the assumed equality of the Σ^- and Σ^+ masses. This interpretation appears unlikely as will be discussed.

B. Σ^- and Σ^+ Masses from an Assumed K^- Mass

We carried through the above procedure using a value of the K^- mass equal to the τ^+ mass $M_{\tau^+} = 965.7 \pm .7\ m_e$[6] and determined values for the Σ^- and Σ^+ hyperon masses. Events $\sigma_{\pi\Sigma 2}$ and K_{MH2} yield the Σ^- hyperon mass, whereas events $\sigma_{\pi\Sigma 2}$ and K_{MH1} yield upper limits for the Σ^+ mass.

The resulting masses are given in Table II and Figures 1 and 2.

Discussion

It is not possible to obtain an accurate energy determination of the pion in these particular colinear events. If the pion energy were known in addition to the range of the dark prong (hyperon) a determination of both the K^- and hyperon masses could be made using only two masses (pion and proton) in the $K^- + H \rightarrow \Sigma^{\pm} + \pi^{\mp}$ reactions. Since only the range of the dark prong is known, we must use three masses and can then determine the fourth mass in the foregoing reaction. An inspection of Table II reveals that if the K^- mass is equal to the τ^+ mass a $\Sigma^- - \Sigma^+$ mass difference of $\geq 14 \pm 6\ m_e$ exists, and the Σ^+ mass determined on this basis is $\geq 2325 \pm 3\ m_e$, which is equal to the Σ^+ mass determined from the range of the proton from the Σ^+ decay at rest. This is evidence for the Σ^+ in event $\sigma_{\pi\Sigma 1}$ to have decayed at rest., in which case the $\Sigma^- - \Sigma^+$ mass difference is then equal to $14 \pm 6\ m_e$. The $\Sigma^- - \Sigma^+$ mass difference results from using the same K^- mass in these four events and the fact that the Σ^- hyperon prongs (which must have come to rest) possesses a shorter range than the Σ^+ hyperon in event $\sigma_{\pi\Sigma 1}$. This determination of the $\Sigma^- - \Sigma^+$ mass difference is insensitive to an exact knowledge of the K^- mass and of the stopping power of the emulsion. This interpretation conforms to the K^- particle as the charge conjugate of the K^+ particle, and there is no theoretical reason for the mass equivalence of the Σ^- and Σ^+ hyperons.

The alternative interpretation of two K^- masses and the equality of the Σ^- and Σ^+ hyperon masses is unlikely, since there would then be two different K^- particles, one K^- which reacts forming hyperons and the other K^- particle which reacts forming Σ^- hyperons. This interpretation although consistent with our data would not conform

Table II

K^-, Σ^-, and Σ^+ Masses from the Reaction:

$$K^- + H \rightarrow \Sigma^{\pm} + \pi^{\mp}$$

Event	Identity of Dark Prong	Case A M_{K^-} using M_{Σ^-} = 2327 ± 3 m_e in m_e	Case B Charged Hyperon Masses using M_{K^-} = M_{Σ^+} = 965.5 ± .7 m_e M_{Σ^+} in m_e	M_{Σ^-} in m_e
$\sigma_{\pi\Sigma 1}$	Σ^+	≤ 966 ± 6	≥ 2325 ± 4	
K_{MH1}	Σ^+, (Σ^-)	≤ 935 ± 5	≥ 2355 ± 4	≥ (2355 ± 4)
$\sigma_{\pi\Sigma 2}$	Σ^-	= 952 ± 5		= 2338 ± 4
K_{MH2}	Σ^-	= 951 ± 7		= 2338 ± 6

to the K^- and K^+ as charge conjugate particles and would be a violation of charge independence.

The possibility that the short range Σ^- prongs in the colinear events are due to the K^- absorption by a proton in the nucleus which undergoes the reaction $K^- + p \rightarrow \Sigma^- + \pi^+$ is unlikely. The chance colinearity of the pion and hyperon from such a reaction is small, and furthermore, the range of the Σ^- hyperon would be even shorter than the observed range unless the Σ^- mass were significantly lower than the Σ^+ mass.

Addendum

Since the first report of this type of event and its interpretation as the K^- absorption by hydrogen in the emulsion at the Pisa Conference in 1955 (7) several additional events have been found and other evidence presented to establish a $\Sigma^- - \Sigma^+$ mass difference. Rosselet (8) and Steinberger (9) have independent types of events which yield a Σ^- mass greater than the Σ^+ mass. Fry (10) has reported two colinear events (the ranges are given in figure 1 and 2 - where they are called Wis 1 and Wis 2). One event gives rise to a heavy prong which emits a proton of $\sim 1660\,\mu$ at the end of its range (Σ^+ decay at rest) (event Wis 2) and another event in which the dark prong ends without the formation of a visible secondary or interaction (Wis 1) consistent with a Σ^- giving rise to a zero prong star. We have also recently observed a colinear event in which the dark prong emits a proton of $\sim 1660\,\mu$ (decay at rest), Berk 1. Ticho [11] (unpublished) has observed

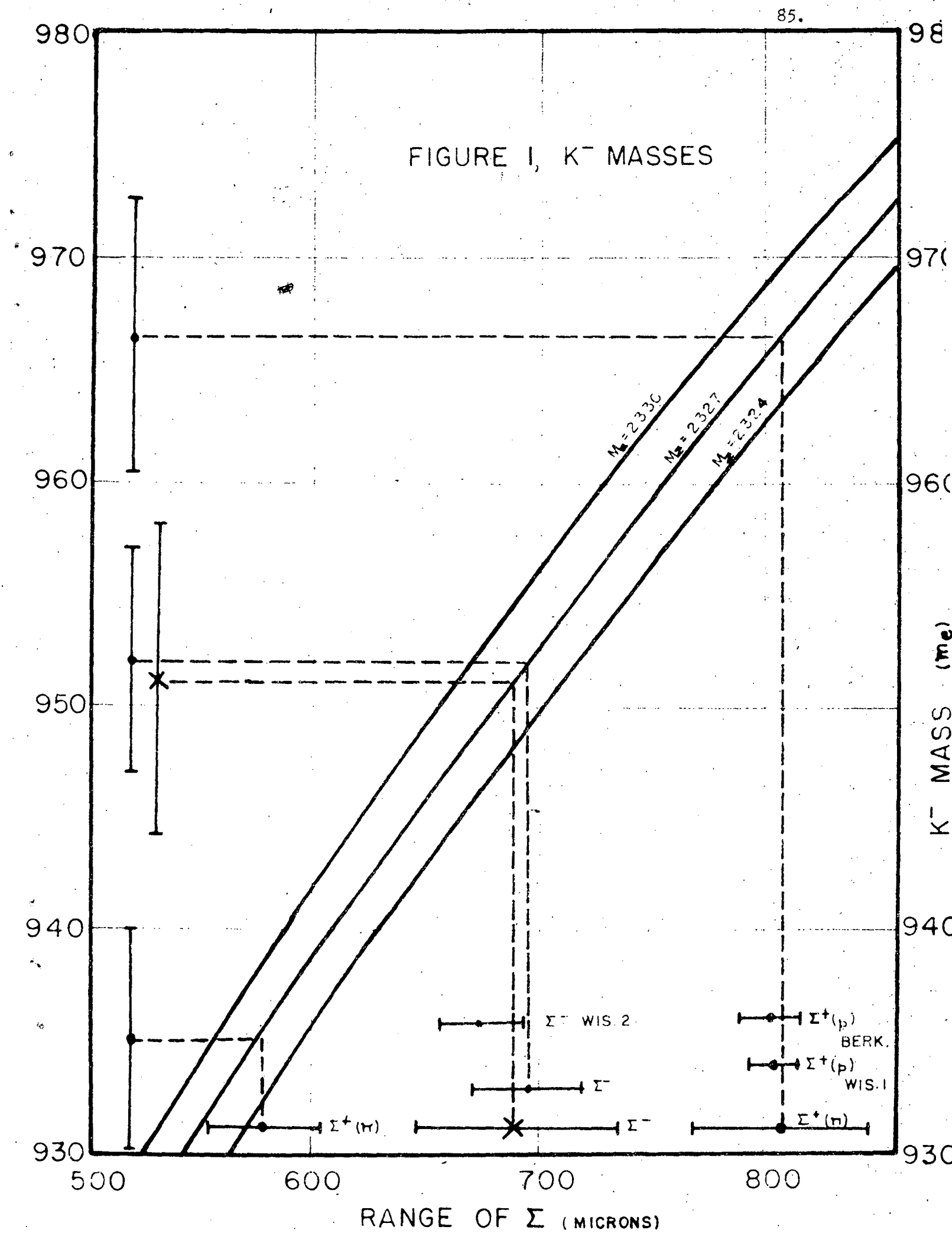
FIGURE I, K⁻ MASSES
980
970
960
950
940
930
500
600
700
800
RANGE OF Σ (MICRONS)
K⁻ MASS (me)
M₁ = 2330
M₂ = 2327
M₃ = 2324
Σ⁻ WIS. 2
Σ⁻
Σ⁻
Σ⁺(π)
Σ⁺(p) BERK.
Σ⁺(p) WIS. 1
Σ⁺(π)

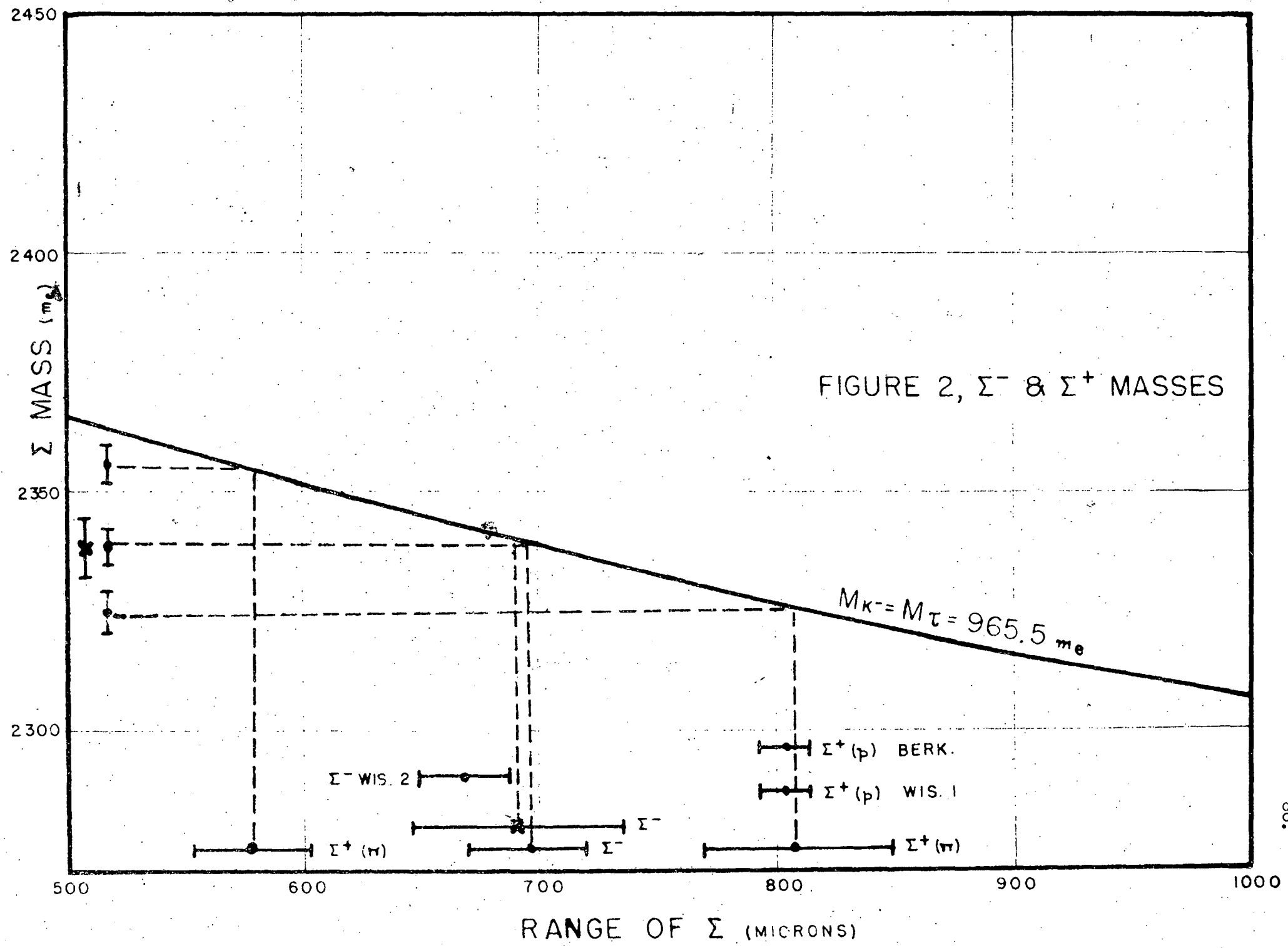
FIGURE 2, Σ⁻ & Σ⁺ MASSES
Σ MASS (mₑ)
2450
2400
2350
2300
500
600
700
800
900
1000
RANGE OF Σ (MICRONS)
Mκ⁻ = Mτ = 965.5 mₑ
Σ⁺ (p) BERK.
Σ⁺ (p) WIS. 1
Σ⁻ WIS. 2
Σ⁻
Σ⁻
Σ⁺ (π)
Σ⁺ (π)

an event where the dark prong has a range of about 700 μ, giving rise to a <u>visible</u> absorption star at the end of its range which is strong evidence for the identification of the dark prong as a Σ^- particle, and lends strong support to the interpretation of the dark prongs as Σ^- particles in the colinear events where the dark prong ends without the formation of a visible absorption star.

These events will be described in more detail in a forthcoming publication.

The preliminary results for all the Berkeley, M. I. T. and Harvard events are:

$$M_{K^-} = 965 \pm 2\ m_e \qquad \text{if } M_{\Sigma^+} = 2327 \pm 1\ m_e \qquad (12)$$

$$M_{\Sigma^-} = 2342 \pm 2\ m_e \qquad \text{if } M_{K^-} = M_{\tau^+} = 965.7 \pm .5\ m_e \qquad (6)$$

and $M_{\Sigma^-} - M_{\Sigma^+} = 14 \pm 2\ m_e$: the mass difference is insensitive to the emulsion density and to the exact value of the K^- mass.

REFERENCES

1. Barkas and Young, UCRL-2579 (Revised), unpublished.
2. Astbury et al. Report of Charged Hyperons, Nuovo Cimento, Supp. XII, 458 (1954).
3. K. M. Crowe and R. H. Phillips, Phys Rev. 96, 470 (1954).
4. Li, Whaling, Fowler, and Lauritsen, Phys Rev. 83, 512 (1951).
5. Rosenfeld and Tripp, Preliminary Report on K^- Hydrogen Events in the Bubble Chamber.
6. Amaldi et al., Report of Committee on Meson, Nuovo cimento Supp. XII, 419 (1954).
7. W. W. Chupp, G. Goldhaber, S. Goldhaber and F. Webb, Proc. of Pisa Conference, 1955, to be published in Nuovo cimento; and U.C.R.L. - 3044.
8. Ph. Rosselet, R. Weill, M. Gailloud, CERN reports, February 1, 1956.
9. J. Steinberger et al., Columbia, Nevis Cyclotron Lab. reports, Nevis 27, May 1956.
10. Fry, Schipps, Snow, Swami and Wold, Phys. Rev. 104, 270 (1956).
11. Private communication from Dr. Ticho
12. Fry, Schnepa, Snow and Swami, Phys. Rev. 103, 226 (1956).

ACKNOWLEDGMENTS

The author wishes to thank Professor Gerson Goldhaber and Dr. Sula Goldhaber for continued interest, encouragement, and many valuable suggestions on all phases of this work. He would also like to acknowledge valuable discussions with Professor Kenneth Watson and Dr. Gosta Ekspong concerning the theoretical interpretation, although the author assumes full responsibility for any errors or mistakes. He is indebted to Dr. Warren Chupp, Dr. Edwin Iloff, and Mr. Joseph Lanmutti for assistance during the experimental phases of this work. The author would like to thank Mrs. C. Toche, Mrs. S. Bostick, Mr. G. M. Wike and Mrs. L. Shaw for their help in scanning the emulsions.

This work was performed under the auspices of the Atomic Energy Commission.

PUBLICATIONS

1. Measurements on K Particles from the Bevatron, Warren W. Shupp, Gerson Goldhaber, S lamith Goldhaber, Stephen J. Goldsack, Joseph E. Lannutti, Francis M. Smith and Francis H. Webb, Phys. Rev. 99 335 - 336, July 1, 1955.
2. Interactions of Negative K Particles at Rest, W. W. Chupp, Gerson Goldhaber, S. Goldhaber, and F. H. Webb, Proc. of Pisa Conf. to be published in Nuovo Cimento, June, 1955.
3. Interaction and Decay of Negative K Particles in Flight, Gerson Goldhaber, Sulamith Goldhaber, Edwin L. Iloff, Joseph E. Lannutti, and Francis H. Webb (Berk) Widgoff, A. Pevsner and D. Ritson, Proc. of Pisa Conf. (June, 1955).
4. The Ratio of K^- Mass to K^+ Mass, Francis H. Webb, Warren W. Chupp. Gerson Goldhaber, and Sulamith Goldhaber, Phys. Rev. 101, 1212 - 1214, February, 1956.
5. K Particle Production at the Bevatron, W. W. Chupp, S. Goldhaber, W. R. Johnson, F. Webb, UCRL 3009 (unpublished).